CHAPTER III

RESULTS AND DISCUSSION

3.1 Sucrose determination

3.1.1 Simple LOC with naked eyes

3.1.1.1 Optimization

3.1.1.1.1 Concentration of bromothymol blue (BTB)

In this study, the concentration of BTB was studied by comparing the differences in percentages of weight by volume (%w/v) of BTB at 0.01, 0.05, 0.10, 0.50, and 1.00 injected into the horizontal channel. This study was done with each of the concentration of sucrose injected into vertical channel. It was found that the migration zone of the BTB at concentrations lower than 1.00% w/v could not be observed clearly. Therefore, BTB of 1.00 %w/v was selected because the migration zone could be detected with naked eyes and a stopwatch.

3.1.1.1.2 pH of borate buffer

BTB is a chemical indicator for weak acids and bases. BTB acts as a weak acid in solution appears yellow at pH below 6.0, blue at pH above 7.6. Its protonated and deprotonated forms are as shown in **Figure 3.1** and bluish green respectively in neutral solution. The blue color was used because this color could be observed clearly through acrylic plastic channel. Therefore BTB was prepared in borate buffer at pH 9.0.

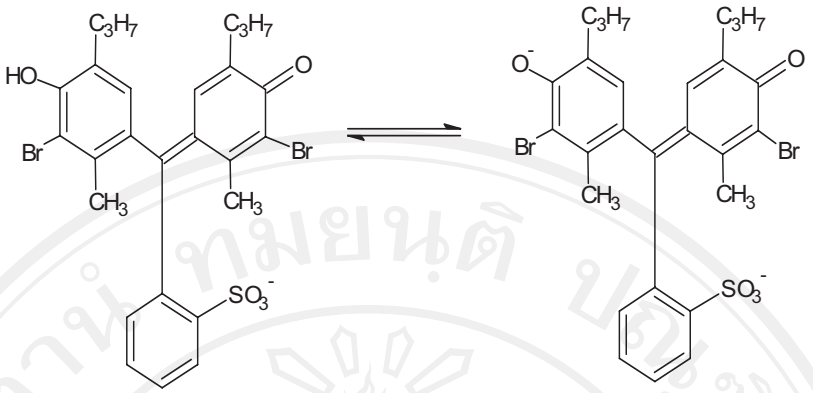

Yellow at pH less than 6.0 Blue at pH more than 7.6

$$HIn + H_2O \rightleftharpoons In^- + H_3O^+$$

HIn represents the protonated form of indicator

In^- represents the unprotonated form of indicator

Figure 3.1 The protonated and deprotonated forms of BTB

3.1.1.1.3 Elevation angle of the chip

In this experiment, the chip was placed with the horizontal plane. Sucrose solution was injected into the vertical channel and BTB indicator into horizontal channel as shown in **Figure 3.2**. The migration times were changed with concentrations of sucrose. Therefore, the elevator of the chip at 0 degree was used in this experiment.

3.1.1.1.4 Detection point

Sucrose solution concentrations of 1.50-2.50 ^{o}Bx were injected into the vertical channel of a simple LOC and mixed with the BTB stream at the channel crossing. The migration times that the product of zones took to reach detection point which was located from the cross away at the distances of 1.00, 1.50, 2.00, 2.50, and 3.00 cm were recorded to build calibration graphs as shown in **Figure 3.2** It was found that the shorter the distance of the detection point from the

channels crossing the better sensitively became as compared to the longer the distances. However, the longer the distance offered better precision in timing. So, the detection point at 1.50 cm was selected for further experiments.

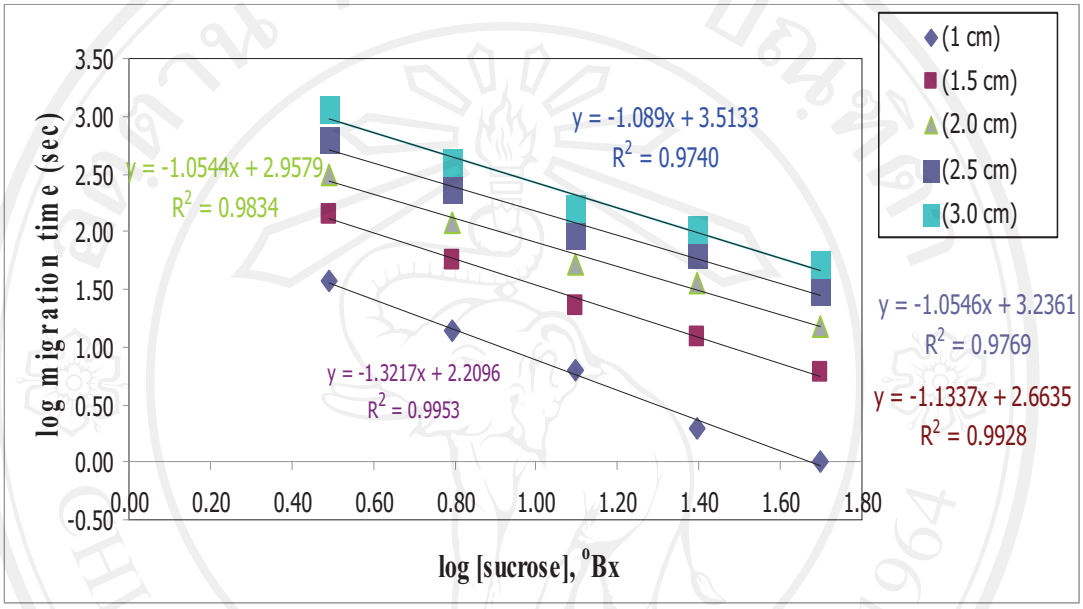

Figure 3.2 The calibration graph obtained when using detection points at various distances from the channels crossing

3.1.1.2 Calibration curve

A linear calibration graph covering the concentration range 10-30 °Bx of sucrose standard solution under investigated conditions was established by plotting the migration time vs. concentration of sucrose as shown in **Figure 3.3 and Table 3.1**. This range of sucrose was studied because the amounts of sucrose generally found in the syrup samples are in the range of 10-30 °Bx.

Table 3.1 Migration time of sucrose standard solutions

[Sucrose],	Detection point, 1.50 cm

°Bx	Migration time, second				SD
	1	2	3	Average	
10.0	33.00	32.00	33.00	32.67	0.58
15.0	26.00	27.00	27.00	26.67	0.58
20.0	19.00	20.00	20.00	19.67	0.58
25.0	15.00	16.00	15.00	15.33	0.58
30.0	11.00	9.00	11.00	10.33	1.15

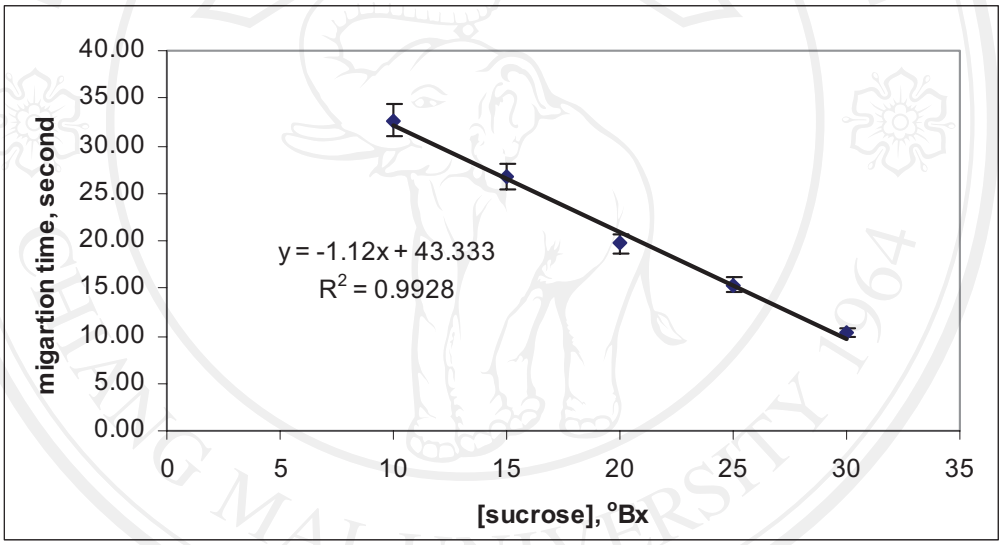

Figure 3.3 Calibration curve of sucrose standard solutions

It should be noted that the calibration graph has negative slope. Increase in sucrose concentration decreased the migration time.

3.1.1.3 Sucrose analysis of real samples

In this study, calibration graph of sucrose was constructed using a simple LOC with naked eyes in the selected optimum conditions. The samples were analyzed directly without any pretreatment. The results are summarized in **Table 3.2**

Table 3.2 Determination of sucrose in the real samples.

Sample	Detection point, 1.50 cm				SD	[Sucrose], ^{o}Bx	
	Migration time, second					Simple LOC	Refractometer
	1	2	3	Average			
s1	10.00	10.00	10.00	10.00	0.00	69	75
s2	14.00	14.00	14.00	14.00	0.00	61	68
s3	10.00	13.00	11.00	11.33	1.53	65	75
s4	13.00	14.00	14.00	13.67	0.58	59	67
s5	22.00	21.00	22.00	21.67	0.58	44	54
s6	13.00	11.00	13.00	12.33	1.15	67	64
s7	10.00	12.00	11.00	11.00	1.00	65	67
s8	20.00	18.00	19.00	19.00	1.00	48	42

The results obtained from the sample LOC method were compared to those obtained from generally used refractometer method. They were in acceptable with refractometer.

3.1.2 Simple LOC with fiber optic spectrophotometer

3.1.2.1 Optimization

3.1.2.1.1 Elevation of the chip

This study depended on turning point (changing of the time based analysis). The preliminary step, peristaltic pump was used to drive continuous flow of the carrier stream (DI water) into the vertical channel. The sucrose solution was injected into the horizontal channel. The elevator of the chip at 0, 10, 30, and 50 degree did not offer any change of turning point, Nevertheless, the elevator of the chip at 60 degree was usable. Therefore, the chip was tilted at angle 60 degree with respect to the horizontal plane in this experiment.

3.1.2.1.2 Detection point

From the previous experiment, the detection point at 1.50 cm on a chip was selected. However, in this experiment was desired to reduce the analysis time. Therefore, the chip was drilled at 1.00 cm away from the channels crossing and fiber optic spectrophotometer was used as the detection unit.

3.1.2.2 Calibration curve and re-study of detection wavelength

Figure 3.4 shows the examples of signals of each sucrose concentration. The time based analysis (turning point) calibration graph of sucrose standard solution is as shown in the **Figure 3.5 and Table 3.3** Linearity of the working range was formed to be 10-50 ^{o}Bx. Different detection wavelengths were investigated (470, 500, 600, and 800 nm). The wavelength at 600 nm was not suitable for analysis. Therefore, the wavelength at 470, 500, and 800 nm were used in the calibration graphs.

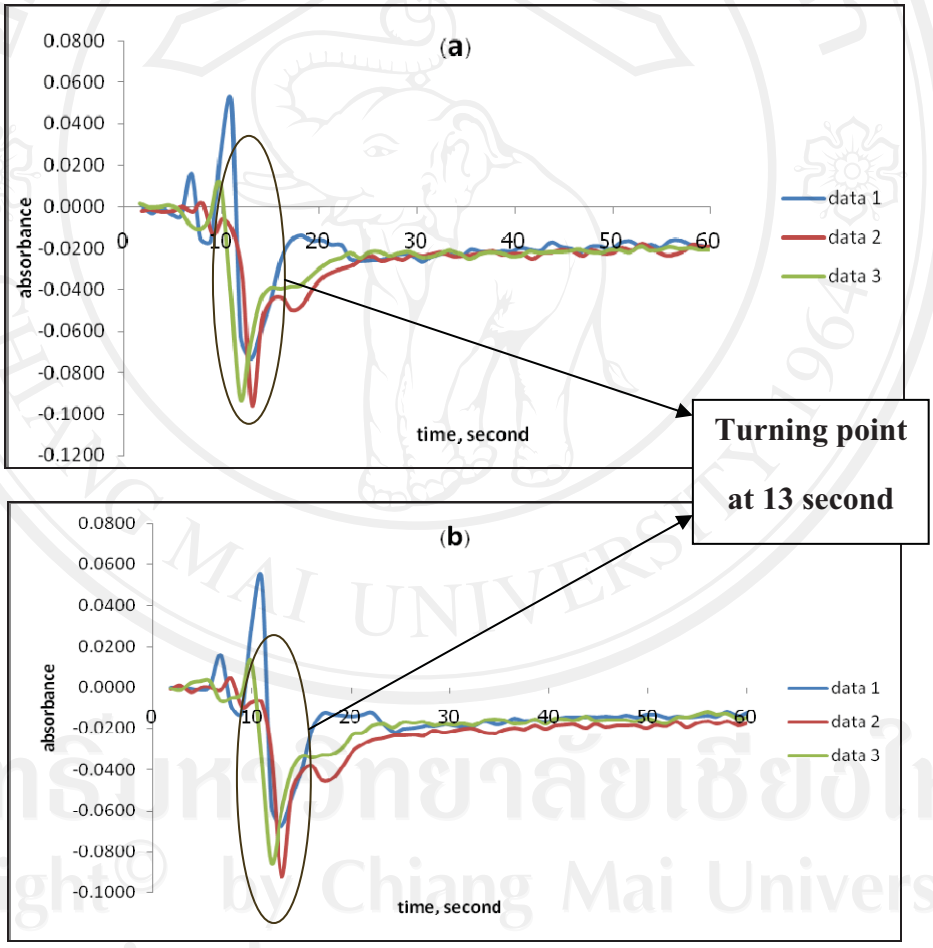

Figure 3.4 Each wavelength of sucrose at 10 ^{o}Bx (a) 470 nm (b) 500 nm

Table 3.3 Turning point of standard sucrose detected at four different wavelengths

[Sucrose], ^{o}Bx	Turning point			
	470 nm	500 nm	600 nm	800 nm

10	13	13	13	13
20	18	18	20	20
30	22	22	18	22
40	25	25	n.d.	25
50	32	32	9	32
67	n.d.	n.d.	n.d.	n.d.

n.d. as no detected

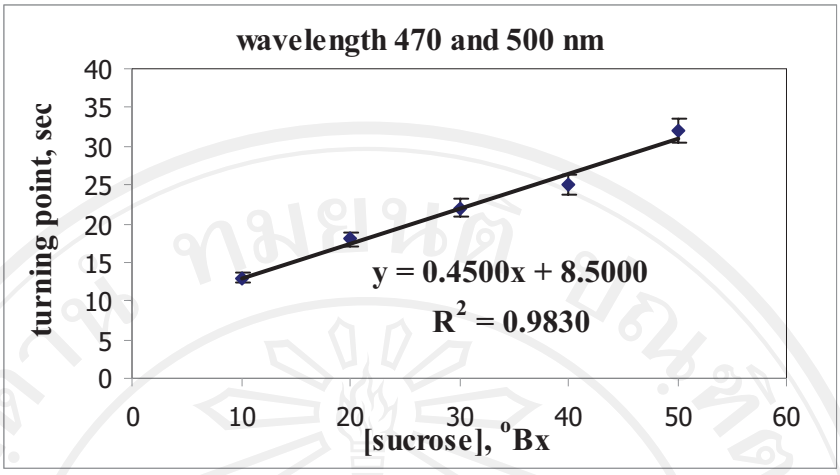

(a)

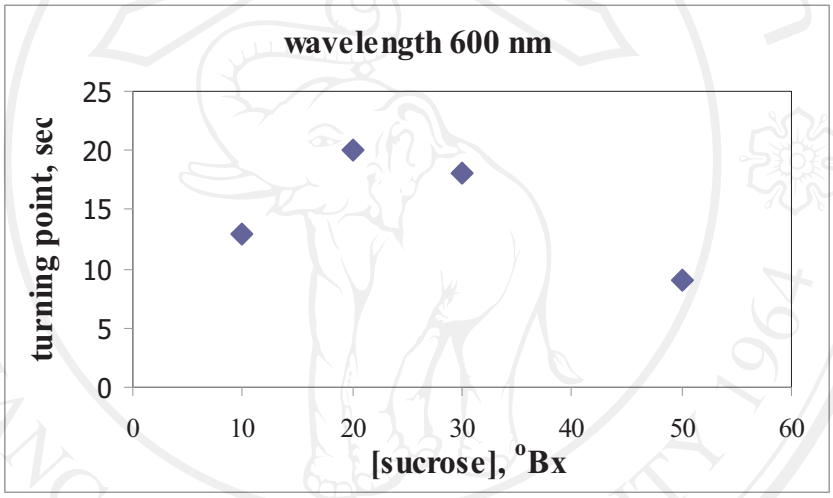

(b)

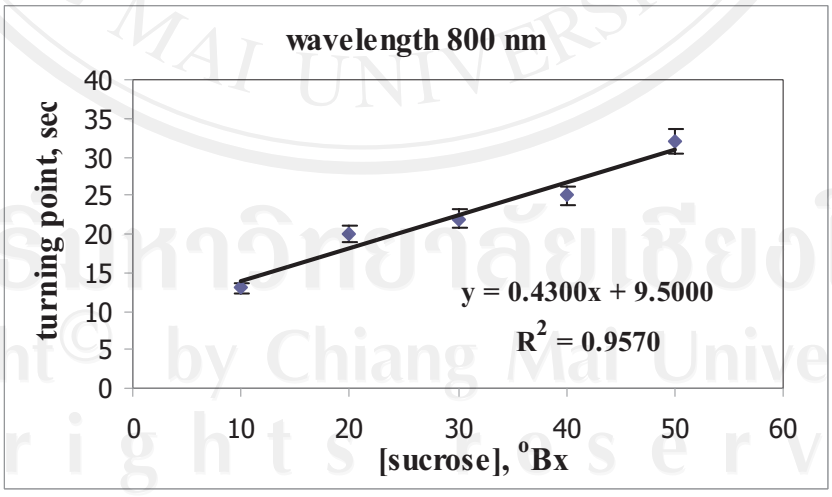

(c)

Figure 3.5 Calibration curve of sucrose concentration of wavelength (a) at 470 and 500 nm (b) at 600 nm (c) at 800 nm

The calibration curve has positive slope because the increasing of sucrose concentration increased the turning point. This may be due to the schlieren effect or refractive index, caused by the light moving through the medium of different densities as a result the direction of light changes.

3.1.2.3 Sucrose analysis in real samples

In this experiment, samples were prepared the same may as previously described when using a simple LOC with naked eyes and some samples were diluted. The results are summarized in **Table 3.4-3.6**. It was found that the results agree well with those obtained by a refractometer.

Table 3.4 Determination of sucrose in real samples at wavelength 470 nm (Simple LOC with fiber optic spectrophotometric set-up)

Type of sample	Turning point, second				SD	[Sucrose], ^{o}Bx			
	Wavelength 470 nm					From equation	Dilution factor	Content	Refractometer
	1	2	3	Average					
s1	22	28	22	24	3.46	34	2.31	80	75
s2	23	23	23	23	0.00	32	2.33	75	68
s3	23	23	23	23	0.00	32	2.26	73	75
s4	22	22	22	22	0.00	30	2.24	67	67
s5	18	18	18	18	0.00	21	2.28	48	54
s6	20	25	25	23	2.89	33	2.41	79	64
s7	n.d.	17	23	18	4.16	22	2.25	57	67
s8	17	17	17	17	0.00	19	2.21	42	42

n.d. as no detected

Table 3.5 Determination of sucrose in real samples at wavelength 500 nm (Simple LOC with fiber optic spectrophotometric set-up)

Type of sample	Turning point, second				SD	[Sucrose], ^{o}Bx			
	Wavelength 500 nm					From equation	Dilution factor	Content	Refractometer
	1	2	3	Average					
s1	22	28	22	24	3.46	34	2.31	80	75
s2	23	23	23	23	0.00	32	2.33	75	68
s3	25	25	25	25	0.00	37	2.26	83	75
s4	22	22	22	22	0.00	30	2.24	67	67
s5	18	18	18	18	0.00	21	2.28	48	54
s6	18	20	20	19	1.15	24	2.41	58	64
s7	15	22	22	20	4.04	25	2.25	67	67
s8	17	17	17	17	0.00	19	2.21	42	42

Table 3.6 Determination of sucrose in real samples at wavelength 800 nm (Simple LOC with fiber optic spectrophotometric set-up)

Type of sample	Turning point, second				SD	[Sucrose], ^{o}Bx			
	Wavelength 800 nm					From equation	Dilution factor	Content	Refractometer
	1	2	3	Average					
s1	22	28	22	24	3.46	34	2.31	78	75
s2	23	23	23	23	0.00	31	2.33	73	68
s3	25	25	25	25	0.00	36	2.26	82	75
s4	22	22	22	22	0.00	29	2.24	65	67
s5	19	19	19	19	0.00	22	2.28	50	54
s6	18	20	20	19	1.15	23	2.41	55	64
s7	23	23	23	23	0.00	31	2.25	70	67
s8	17	17	17	17	0.00	17	2.21	38	42

3.1.3 FI system with fiber optic spectrophotometer

3.1.3.1 Calibration curve and wavelength

The calibration graphs were plotted between concentration of sucrose standard solution and turning point at each wavelength (470, 500, 600, and 700 nm). The absorbance signals were recorded with the E-DAQ program as shown in the **Table 3.7.** The wavelength of 700 nm was not appropriated for the analysis.

Table 3.7 Peak area of standard sucrose detected at three different wavelengths

[Sucrose], ^{o}Bx	Peak area		
	Wavelength, nm		
	470 nm	500 nm	600 nm
10	0.2580	0.2097	0.1053
20	0.3615	0.3020	0.1358
30	0.5304	0.4373	0.2387
40	0.7208	0.6226	0.5644
50	0.9832	0.8333	0.7217
67	1.6097	1.3589	0.9983

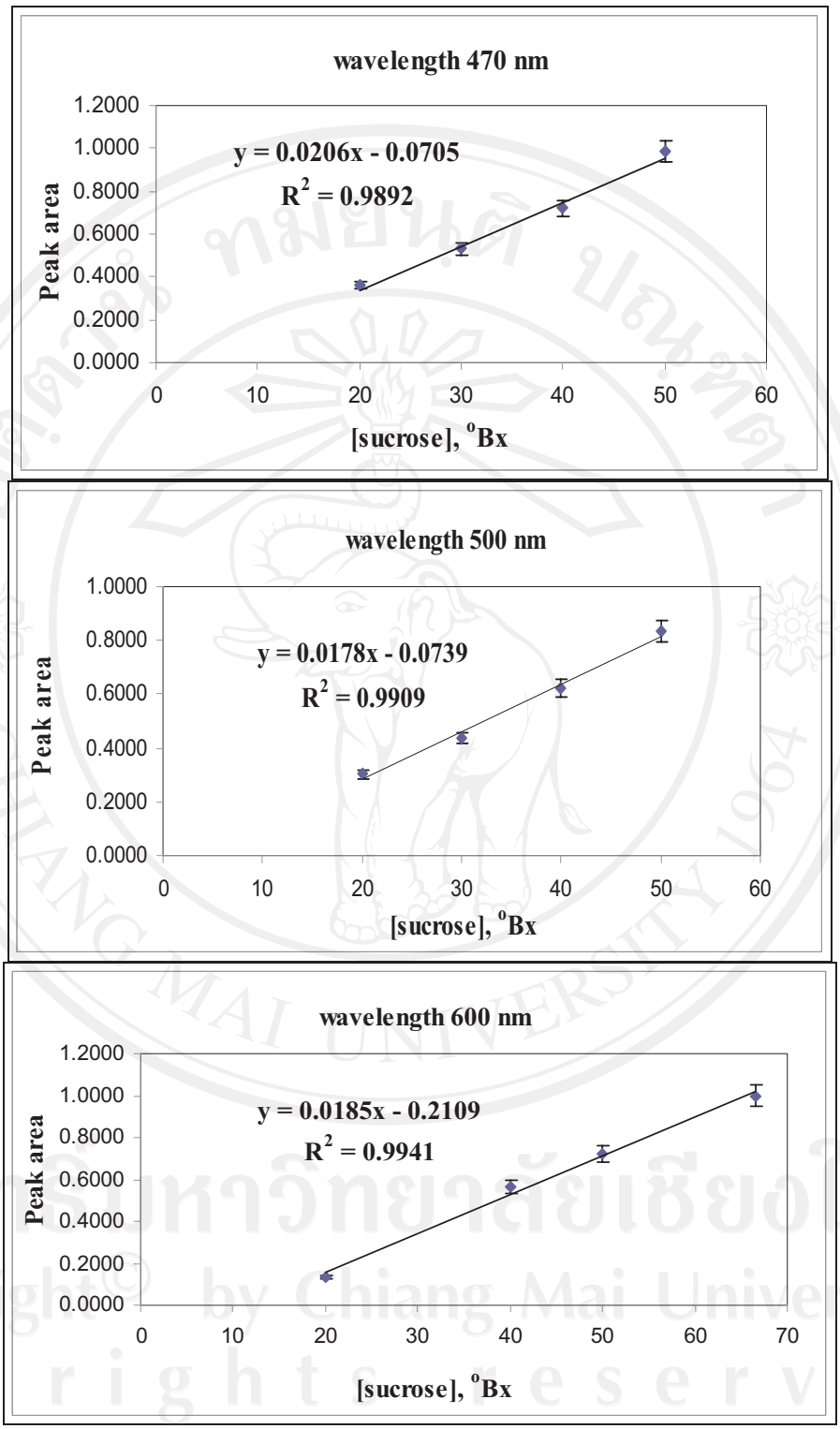

Figure 3.6 The calibration curve of sucrose concentration of each wavelength

It was found that calibration graphs have positive slopes because increasing concentration of sucrose increased the peak area due to the changes of refraction of light in medium of different densities of sucrose.

3.1.3.2 Real samples

The determination of sucrose is based on the peak areas of various sucrose concentrations. Samples were diluted to appropriate concentrations to construct a calibration curve. The results are summarized in **Table 3.8-3.10**. Quantities of sucrose in real samples found in the proposed method were well agreed with a refractometer method.

Table 3.8 Determination of sucrose in real samples at wavelength 470 nm (FIA set-up)

Sample	[Sucrose], ^{o}Bx								
	FIA procedure								Refracto-meter
	Peak area (Wavelength 470 nm)					Value from calibration	Dilution factor	Content	
	1	2	3	Average	SD				
s1	0.618	0.5853	0.5327	0.5787	0.04	32	2.31	73	75
s2	0.4924	0.563	0.5633	0.5396	0.04	30	2.33	69	68
s3	0.6074	0.521	0.5451	0.5578	0.04	30	2.26	69	75
s4	0.6227	0.5083	0.5192	0.5501	0.06	30	2.24	67	67
s5	0.467	0.4491	0.4204	0.4455	0.02	25	2.28	57	54
s6	0.5495	0.5155	0.5285	0.5312	0.02	29	2.41	70	64
s7	0.2797	0.3088	0.3003	0.2962	0.01	18	2.25	40	67
s8	0.3854	0.3823	0.4582	0.4086	0.04	23	2.21	51	42

Table 3.9 Determination of sucrose in real samples at wavelength 500 nm (FIA set-up)

Sample	[Sucrose], °Bx								
	FIA procedure								
	Peak area (Wavelength 500 nm)					Value from calibration	Dilution factor	Content	Refracto-meter
	1	2	3	Average	SD				
s1	0.5346	0.4944	0.4384	0.4891	0.05	32	2.31	73	75
s2	0.4149	0.4817	0.4717	0.4561	0.04	30	2.33	69	68
s3	0.5097	0.4362	0.4642	0.47	0.04	30	2.26	69	75
s4	0.5078	0.419	0.4255	0.4508	0.05	29	2.24	66	67
s5	0.4137	0.4069	0.3813	0.4006	0.02	27	2.28	61	54
s6	0.5084	0.4624	0.4896	0.4868	0.02	32	2.41	76	64
s7	0.2167	0.2625	0.2472	0.2421	0.02	18	2.25	40	67
s8	0.3352	0.3381	0.4023	0.3585	0.04	24	2.21	54	42

Table 3.10 Determination of sucrose in real samples at wavelength 600 nm (FIA set-up)

Sample	[Sucrose], °Bx								
	FIA procedure								
	Peak area (Wavelength 600 nm)					Value from calibration	Dilution factor	Content	Refracto-meter
	1	2	3	Average	SD				
s1	0.3859	0.3625	0.3496	0.366	0.02	31	2.31	72	75
s2	0.2885	0.3006	0.3639	0.3177	0.04	28	2.33	67	68
s3	0.3916	0.3703	0.3334	0.3651	0.03	31	2.26	70	75
s4	0.402	0.2933	0.3319	0.3424	0.06	30	2.24	67	67
s5	0.1714	0.174	0.1622	0.1692	0.01	20	2.28	47	54
s6	0.2005	0.1811	0.1856	0.189	0.01	22	2.41	52	64
s7	0.0758	0.1299	0.0866	0.0974	0.03	17	2.25	37	67
s8	0.1572	0.1612	0.2296	0.1827	0.04	21	2.21	47	42

3.1.4 Evaluation of the proposed method for determination of sucrose

The determinations of sucrose in real samples of all methods at each wavelength as were summarized in **Table 3.11**.

Table 3.11 Comparisons of all proposed methods

Type of sample	[Sucrose], ^{o}Bx							
	FIA-USB 2000 Wavelength (nm)			LOC-USB 2000 Wavelength (nm)			LOC-naked eyes	Refracto-meter
	470	500	600	470	500	800		
s1	73	73	72	80	80	78	69	75
s2	69	69	67	75	75	73	61	68
s3	69	69	70	73	83	82	65	75
s4	67	66	67	67	67	65	59	67
s5	57	61	47	48	48	50	44	54
s6	70	76	52	79	58	55	67	64
s7	40	40	37	49	56	70	65	67
s8	51	54	47	42	42	38	48	42

The table indicates that the proposed methods demonstrated for the suitability for sucrose assay.

3.2 Fe (II) determination

3.2.1 Reaction study

In this study, the determination of Fe (II) was selected to evaluate the performance of the simple LOC with fiber optic spectrophotometer. Fe (II) reacted with phenanthroline chelated at the ratio of 1 Fe: 3 phenanthroline to form an orange-red complex as shown in the reaction **Figure 3.7**. This phenanthroline complexing reagent is specific for Fe (II) only. However, because the instability of Fe (II) that can easily changed easily to the ferric form when in contact with air, the determination of Fe (II) required treatment in concentrated HCl. It may need to be done at this time of sample collection. Fe (II) will be measured to appropriate with quantitative analysis.

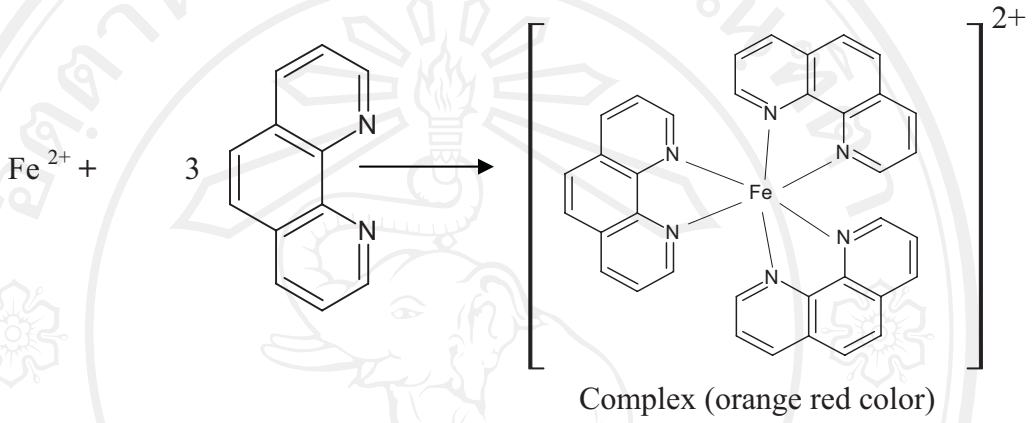

Figure 3.7 The formation of $[Fe(phen)_3]^{2+}$ complex

3.2.2 Simple LOC with fiber optic spectrophotometer

3.2.2.1 Absorption spectrum

The orange-red colored complex spectra of Fe (II) and phenanthroline were recorded in order to investigate the optimum wavelength to monitor the complexation reaction. The spectrum of the colored complex has maximum peak at 510 nm as shown in **Figure 3.8.** When this colored complex was included by injecting Fe (II) into the vertical channel and then, 1,10-phenanthroline was injected into horizontal channel. Therefore, the wavelength at 510 nm was selected to determine Fe (II) in the groundwater and ponds water samples.

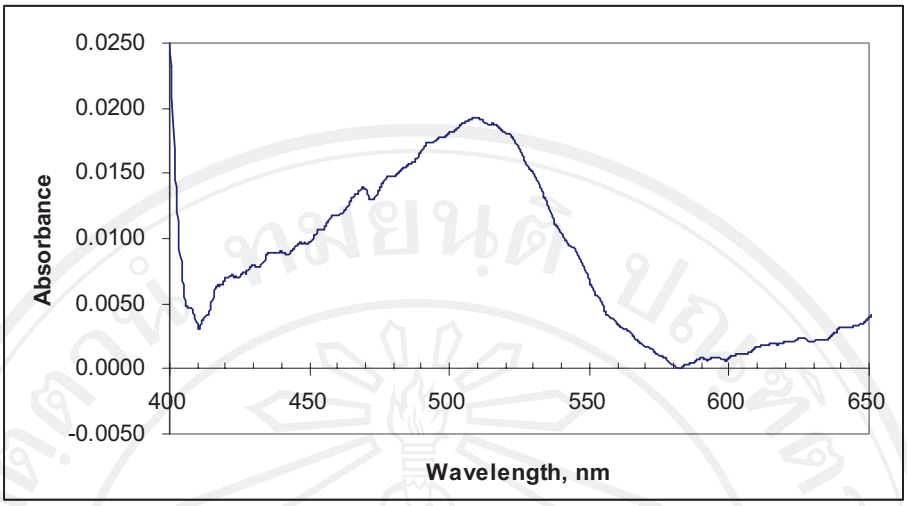

Figure 3.8 Absorption spectra of the orange-red colored complex

3.2.2.2 Elevation of the chip

In this experiment, the chip was placed plot with respect to the horizontal channel.

3.2.2.3 Calibration curve

The calibration curve was constructed using Fe (II) standards (0.03-1.00 ppm) and 1,10-phenanthroline at a maximum wavelength 510 nm, as shown in **Figure 3.9** and **Table 3.12**.

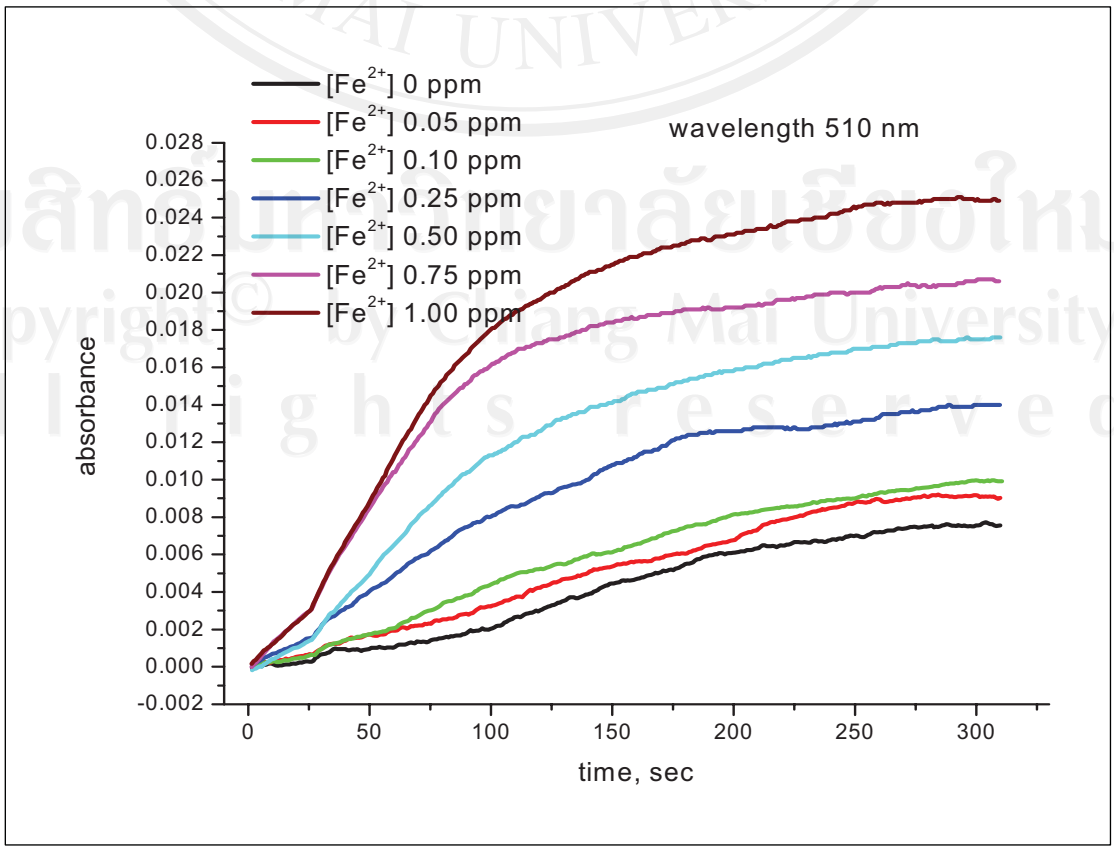

Figure 3.9 The absorbance against time curve of $[Fe(phen)_3]^{2+}$ at wavelength 510 nm

Table 3.12 Calibration data of orange-red complex by using the proposed method

$[Fe^{2+}]$, ppm	Absorbance		Slope	
	1	2	1	2
0	0.0000	0.0000	0.00E+00	0.00E+00
0.03	0.0008	n.d.	-7.46E-06	n.d.
0.05	0.0012	0.0017	2.01E-05	8.63E-06
0.10	0.0022	0.0029	2.66E-05	3.48E-05
0.25	0.0054	0.0060	4.95E-05	6.14E-05
0.50	0.0079	0.0093	1.32E-04	1.06E-04
0.75	0.0124	0.0128	1.77E-04	1.56E-04
1.00	0.0169	0.0175	2.13E-04	1.99E-04
Equation of linearity	y = 0.0163x + 0.0004	y = 0.0166x + 0.0009	y = 0.0002x + 0.0000	y = 0.0002x + 6E-06
R-square (R^2)	0.9941	0.9916	0.9850	0.9933

From the calibration data can be estimated the absorbance value of each Fe (II) concentrations by plotting graph between absorbance/slope versus Fe (II) concentrations at 300 second as shown in **Figure 3.10**

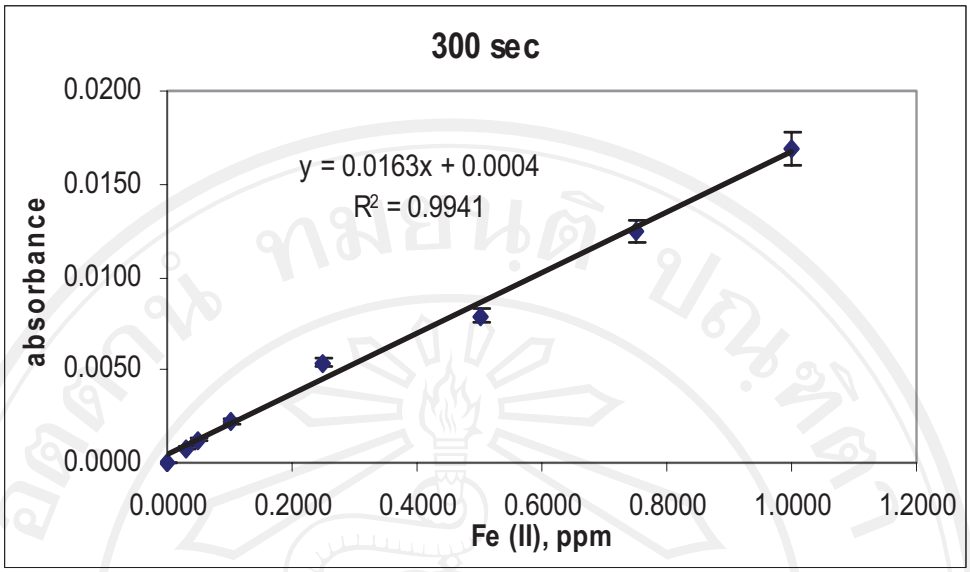

Figure 3.10 Calibration curve between Fe (II) and absorbance/slope of $[Fe(phen)_3]^{2+}$ at wavelength 510 nm

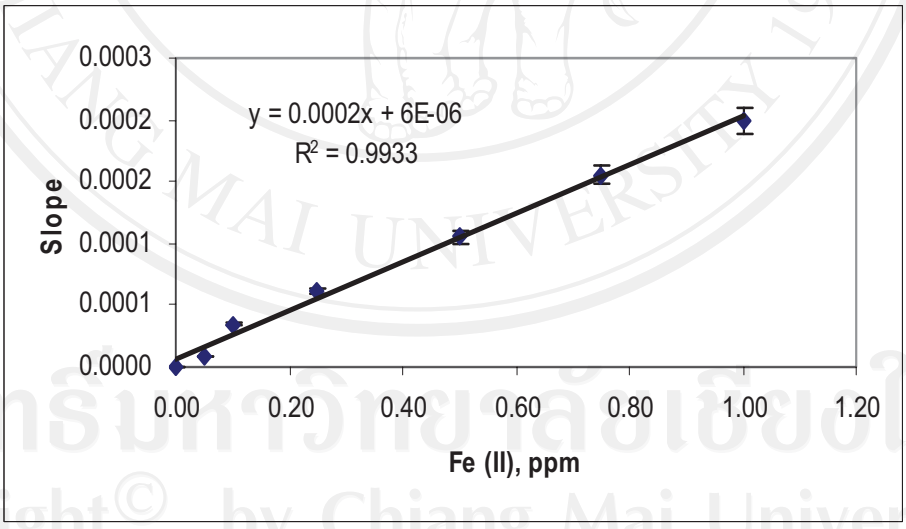

Figure 3.10 (continued)

The equation of the calibration graph was used to determine Fe (II) in the different range. So the determination of Fe (II) should be chosen the suitable ranges with each sample.

The calibration graph has positive slope because the increasing of Fe (II) concentration increased the absorbance/slope of the reaction zone. According to the basic principle of the method (Beer's law) is the quantitative basis for the following determinations.

3.2.2.4 Evaluation of a simple LOC

In this study, the linearity of equation was obtained using operational condition selected from optimization. This sample was treated in concentrated HCl. Some samples (**Table 3.13**) may be diluted to appropriate the range of analysis.

Table 3.13 Determination of Fe (II) in the groundwater and water ponds

Type of sample	Concentration of ferrous iron, ppm		
	The proposed method		The standard method
	Using absorbance	Using slope	
s1	n.d.	n.d.	n.d.
s2 diluted 25 fold	17.82	19.54	18.14
s3	n.d.	n.d.	n.d.
s4	n.d.	n.d.	n.d.
s5	n.d.	n.d.	n.d.
s6	n.d.	n.d.	n.d.
s7 diluted 25 fold	7.07	6.42	7.51
s8	n.d.	n.d.	n.d.
s9	0.84	0.51	0.83
s10	n.d.	n.d.	n.d.

n.d. as no detected

The results were that the equation from calibration graph able to determine Fe (II) in the groundwater and water ponds. Whereon, water ponds will have the amount of Fe (II) less than the range of analysis that a simple LOC can not

be analyzed. In a part of the sample from the groundwater will be have high Fe (II) content so, it have to dilute this sample to be in the range selected for analysis. The results will be confirmed with the UV-VIS spectrophotometric method. It can be accepted for some samples in which suitable for the range of analysis.

In the samples containing less the amount of Fe (II) can also be studied using the standard addition method in the next step.

3.2.2.5 Standard addition

The orange-red colored formation of Fe (II) and 1,10-phenanthroline was studied to make the standard addition. This experiment will be used the same conditions that was optimized in the calibration graph. The effects of matrices were tested by spiking Fe (II) standard solutions of different concentrations (0, 0.10, 0.50, and 1.00 ppm) to gain the final added concentrations into 10 ml of sample. The dilution factor was used equal to 2.5 to determine Fe (II) in real samples.

The absorbance versus time curve of each samples were obtained. It was found that the curve of complex formation has tended to increase rapidly until reach steady state. As can be seen in the **Figure 3.11** for studied interfering species and percent recoveries were observed.

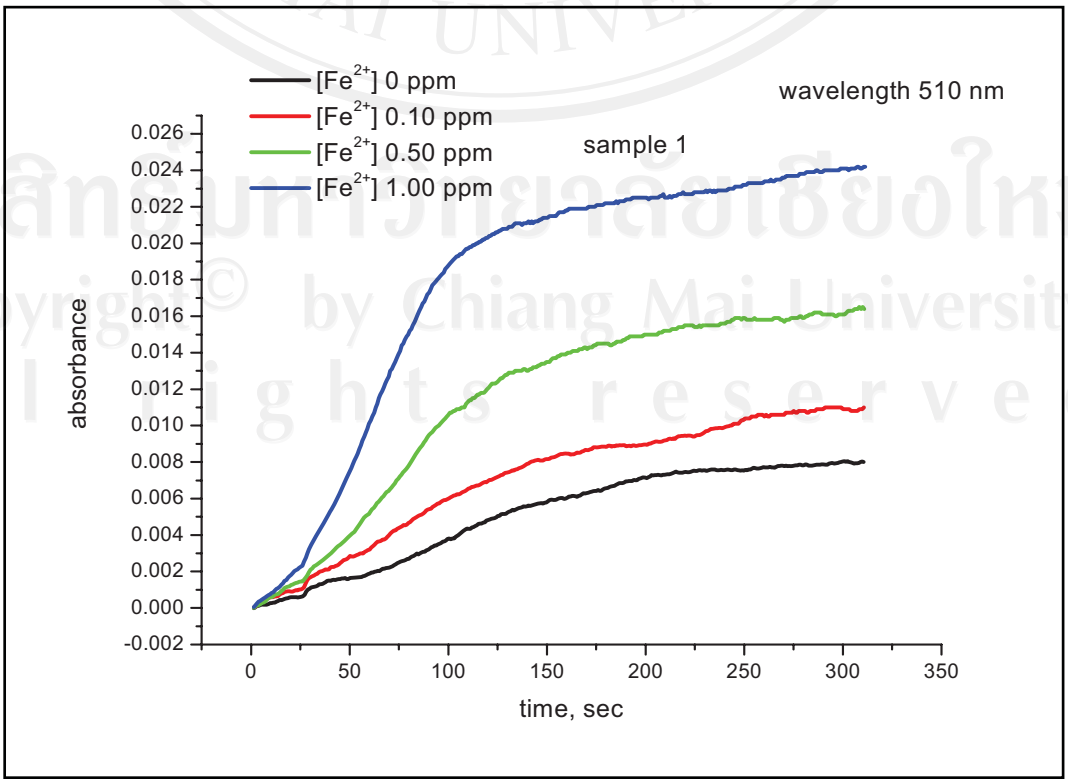

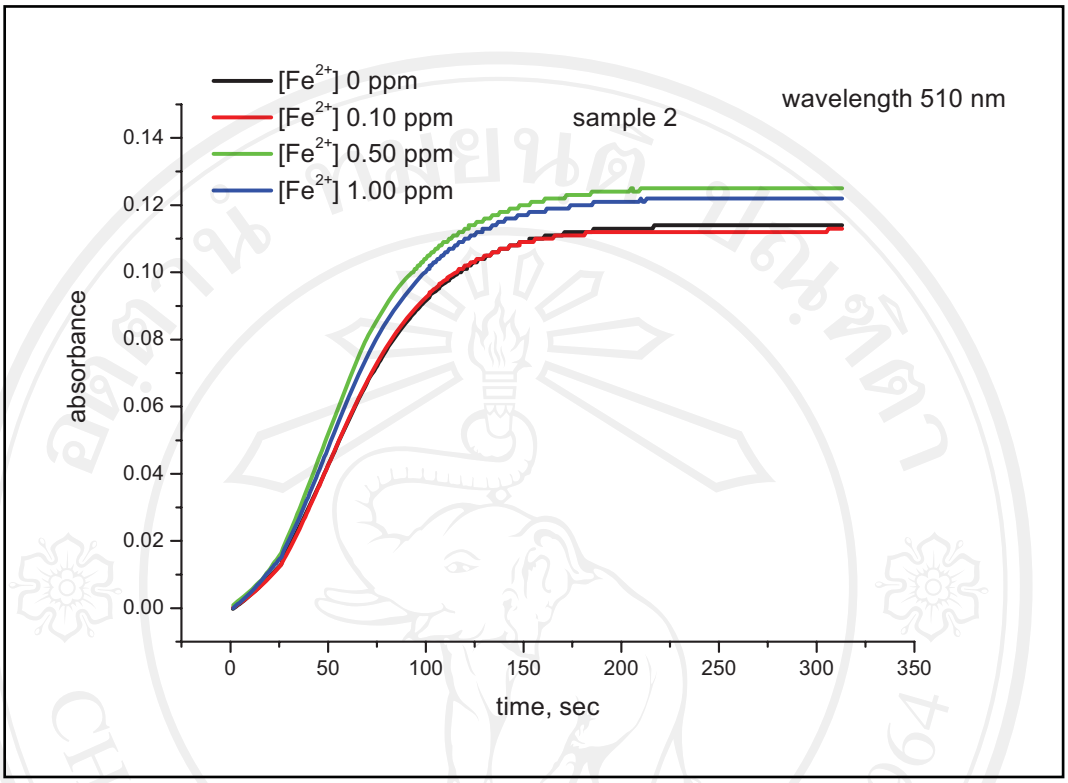

Figure 3.11 Standard addition of sample 1-10

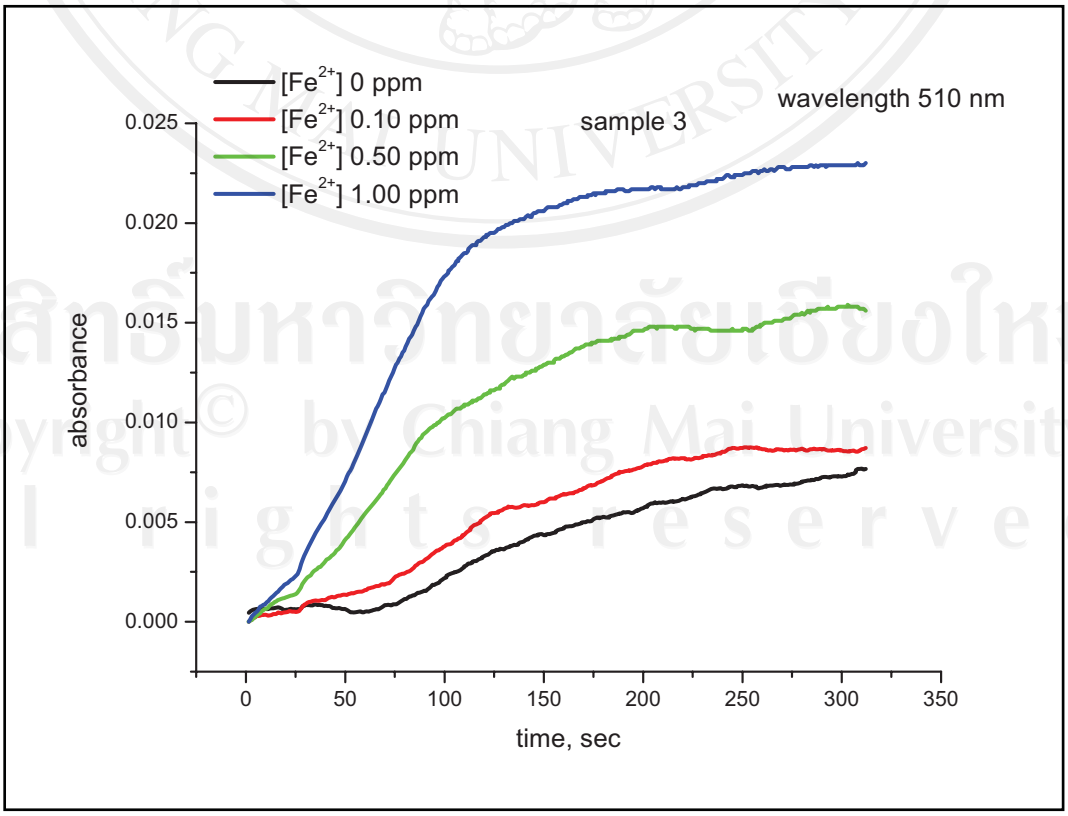

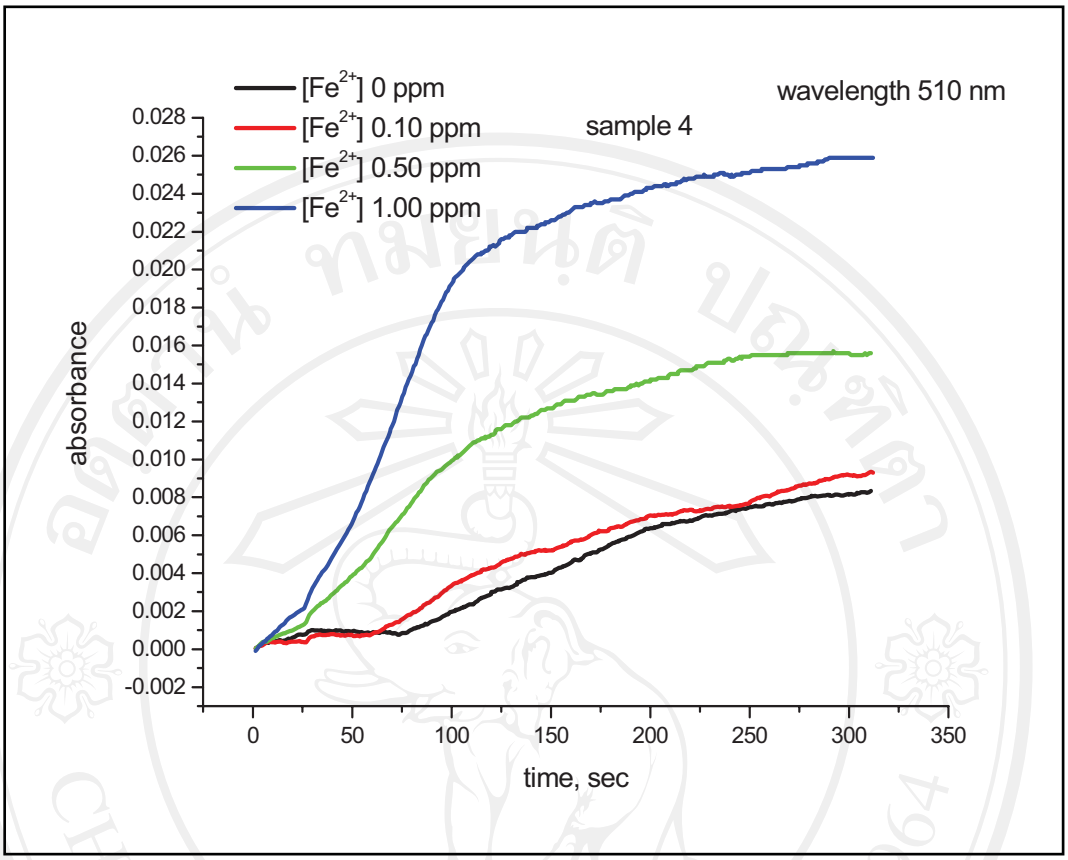

Figure 3.11 (continued)

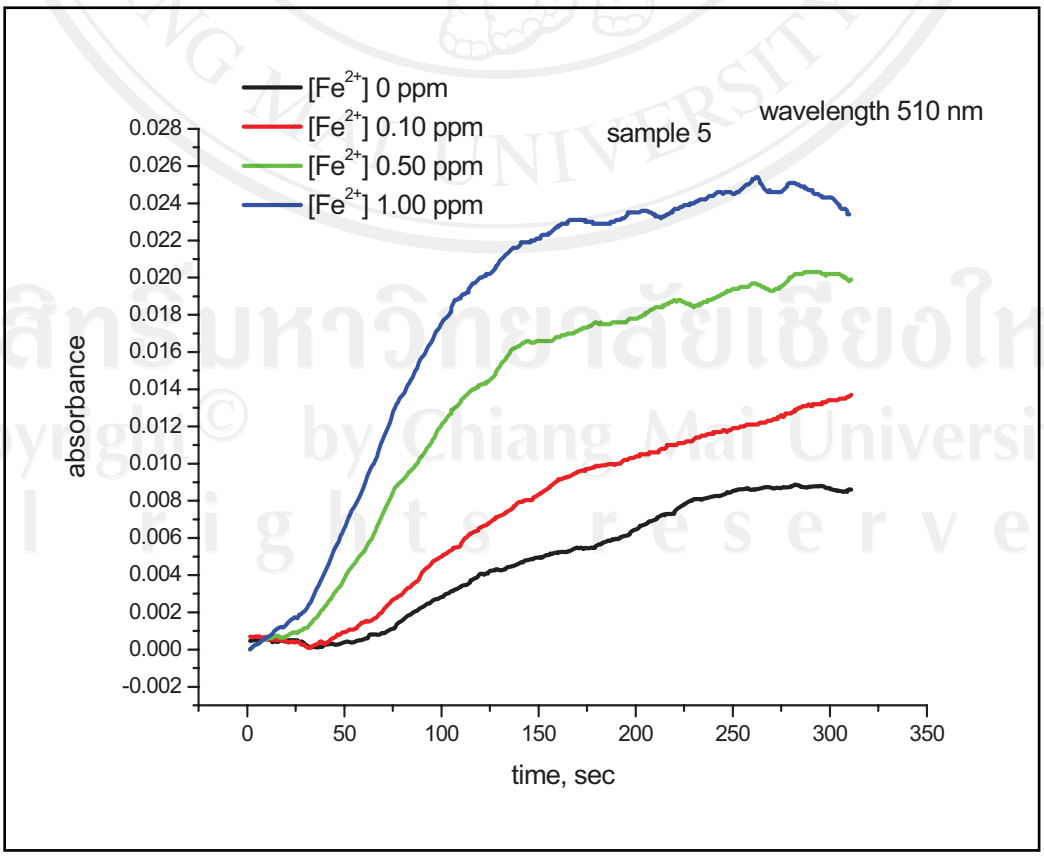

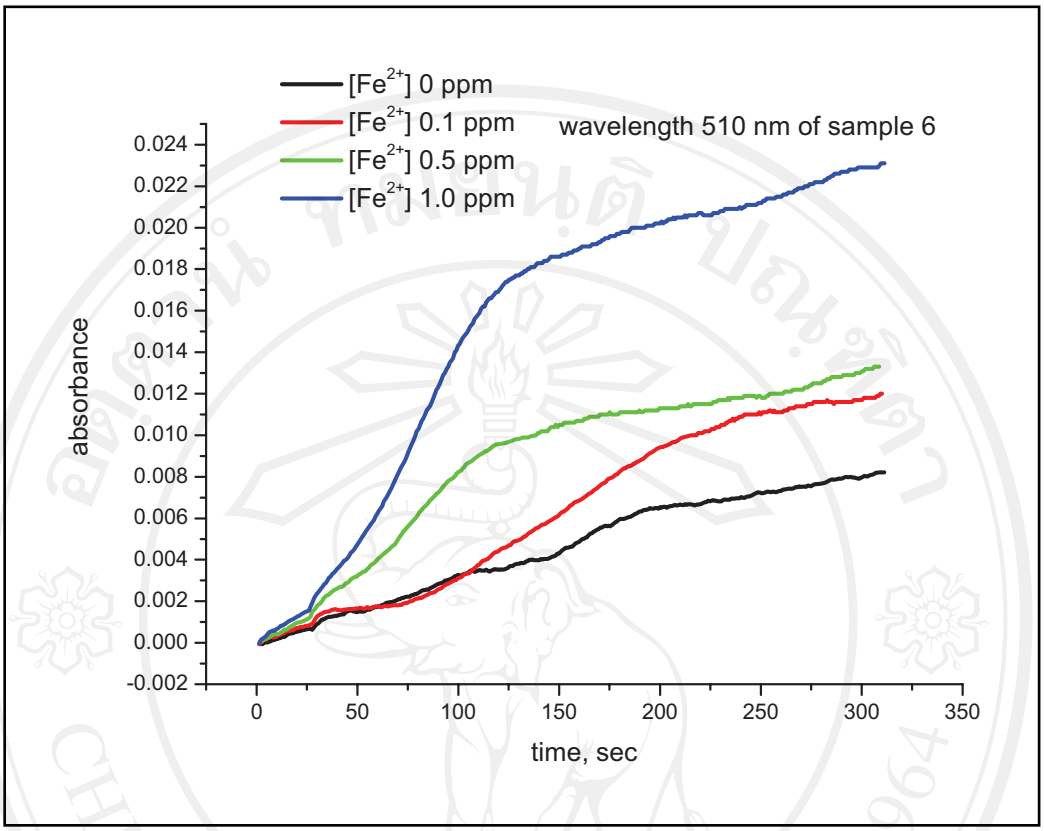

Figure 3.11 (continued)

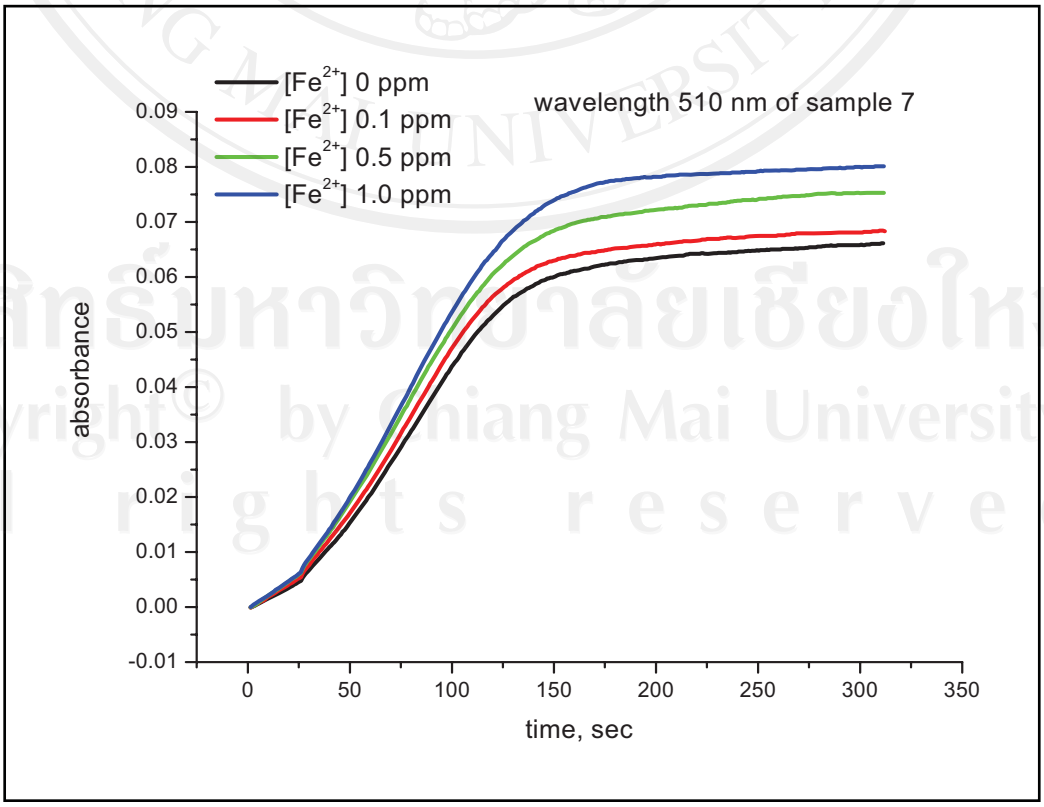

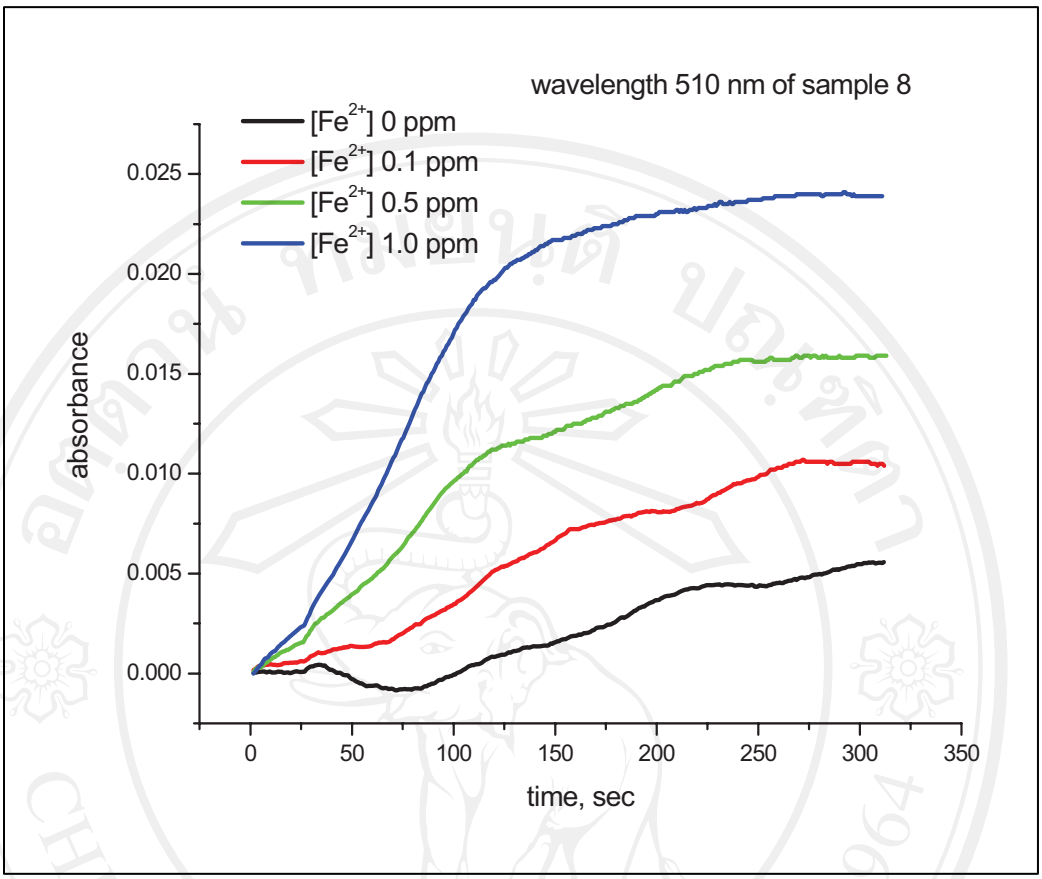

Figure 3.11 (continued)

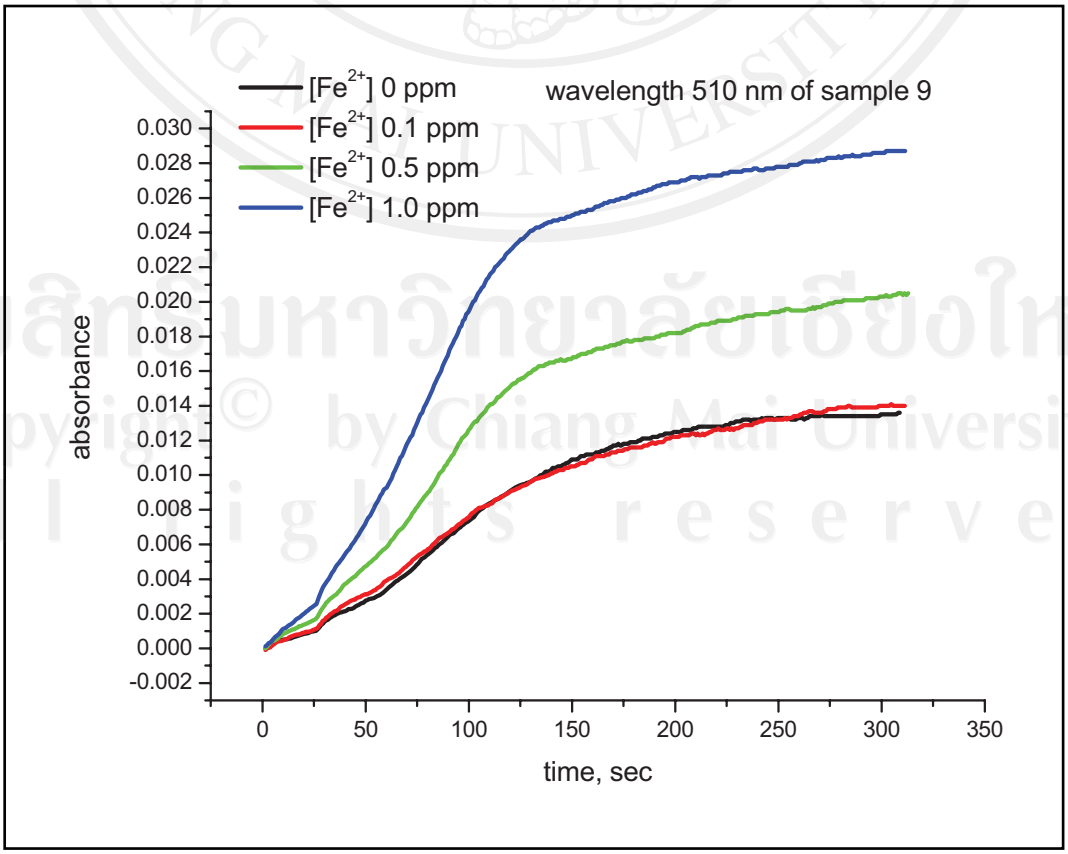

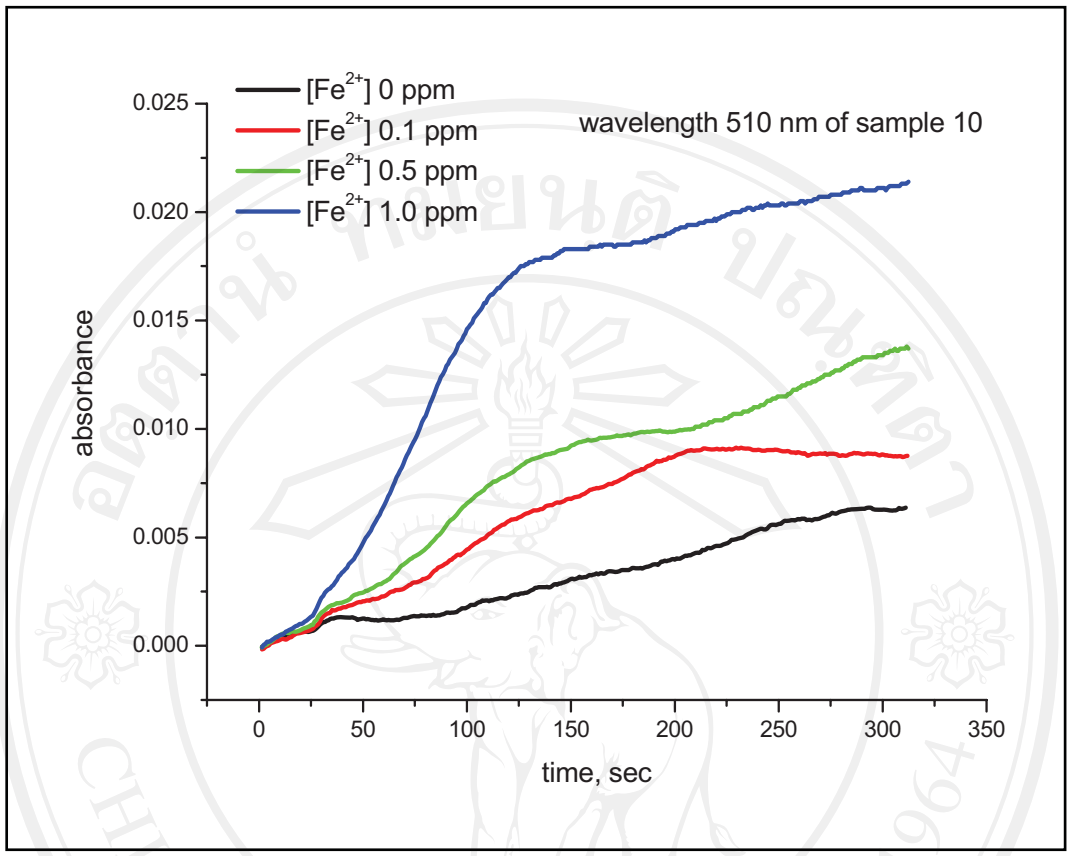

Figure 3.11 (continued)

Percent recoveries were calculated from the results obtained from the standard curve as compared to the expected value from calculation. As can be summarized in **Table 3.14** and **Figure 3.12** were obtained.

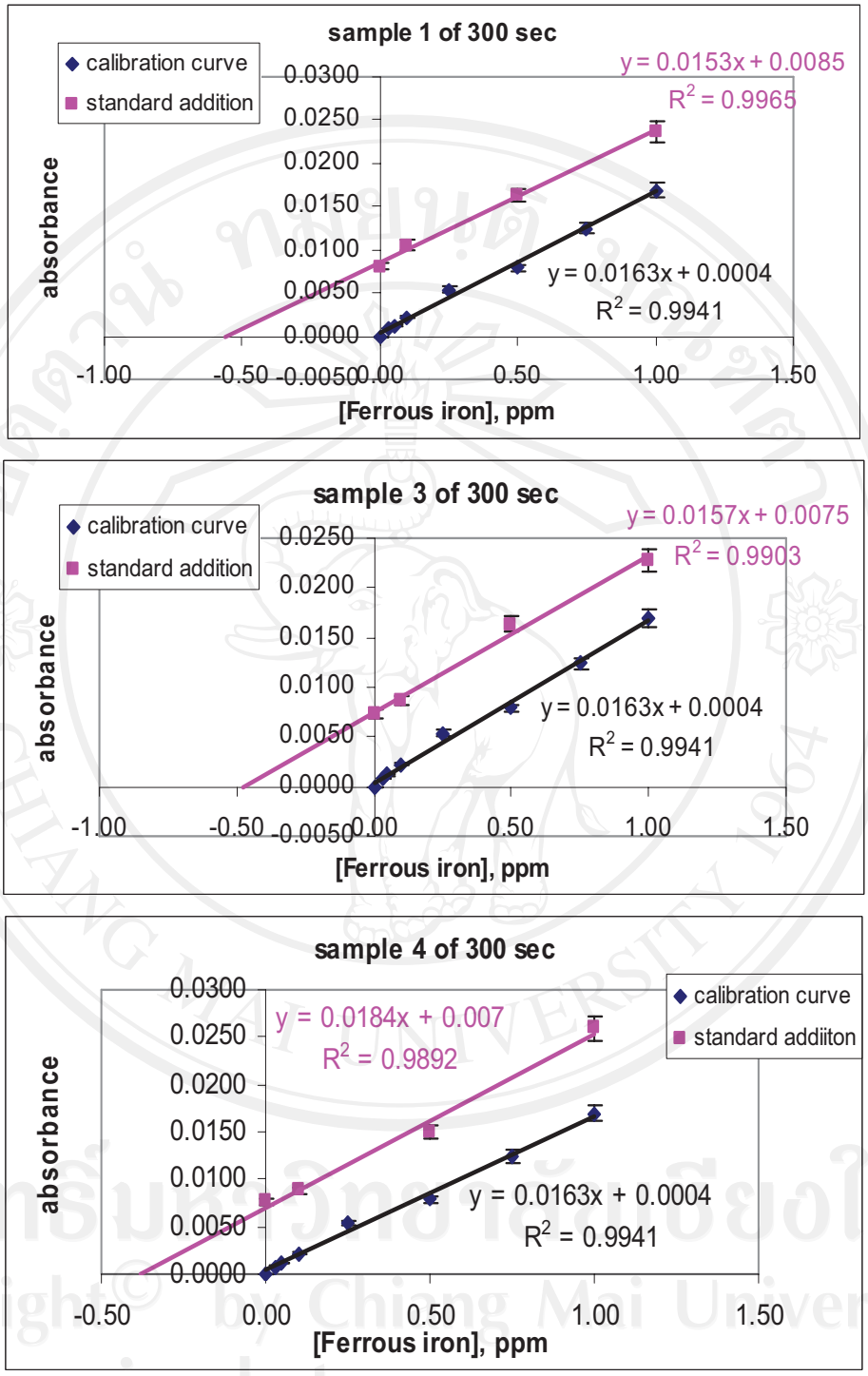

Figure 3.12 Standard addition curve as compared to calibration curve of all samples

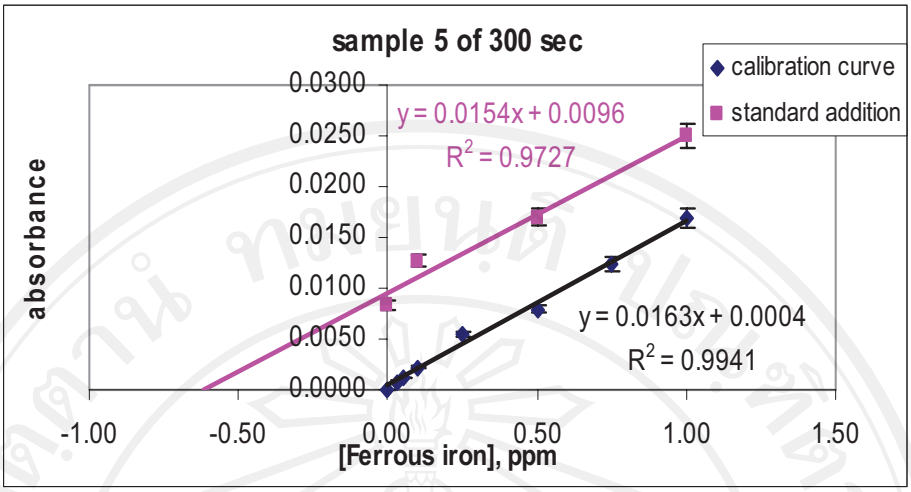

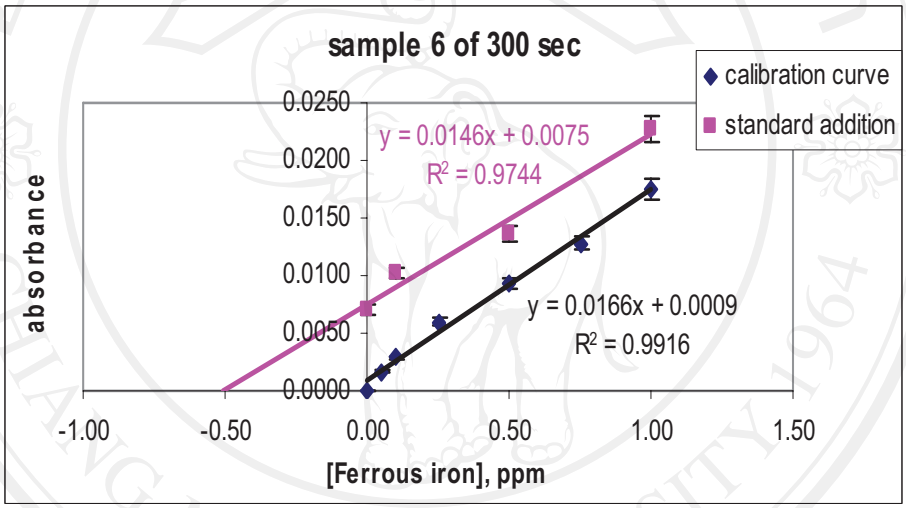

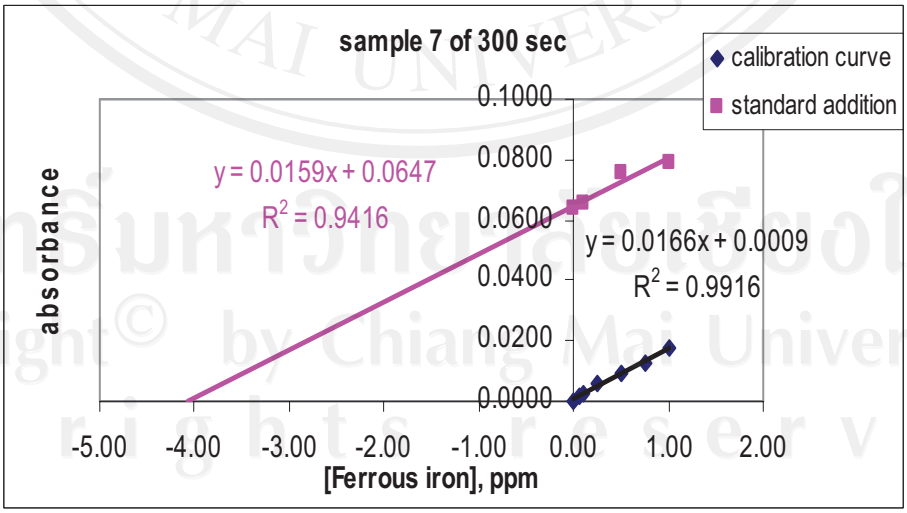

Figure 3.12 (continued)

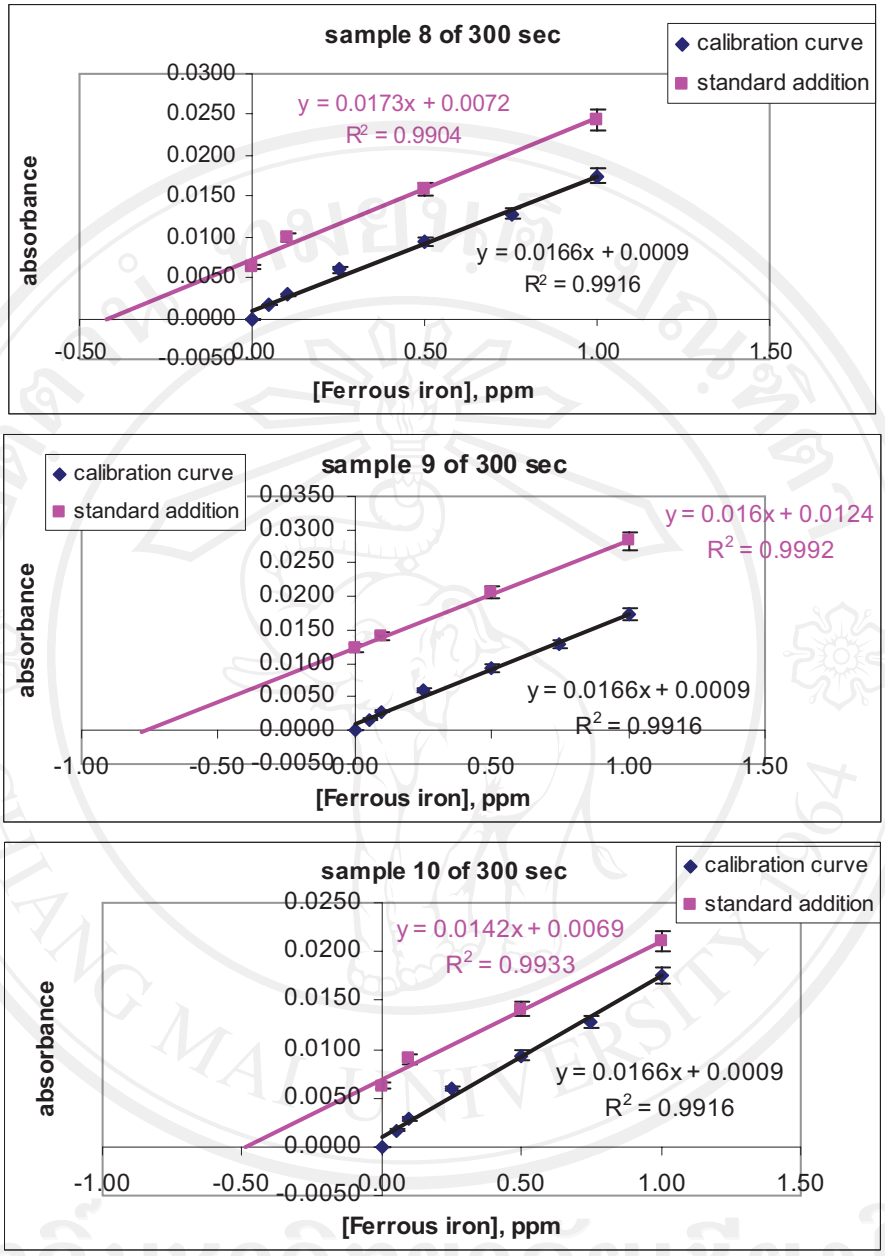

Figure 3.12 (continued)

The results were that effects of interfering substances were investigated and no interference was observed for sample 1-9. It was shown that interfering effect in the sample had not interfere with the range of analysis in order to the preliminary of treatment sample can be eliminated another effect of interference. And then, the sample 10 is unclear what matrices may cause error in the real sample. Determination of Fe (II) and percent recoveries in **Table 3.14** was summarized.

Table 3.14 Determination of Fe (II) and percent recoveries

Type of sample	Concentration of Fe (II), ppm	% Recovery	Spiked standard, ppm
s1	1.39	96	1.00
s2	n.d.	n.d.	n.d.
s3	1.19	94	1.00
s4	0.95	112	1.00
s5	1.56	96	1.00
s6	1.28	94	1.00
s7	10.17	92	1.00
s8	1.04	109	1.00
s9	1.94	97	1.00
s10	1.21	97	1.00

n.d. as no detected

3.2.3 Visible spectrophotometry

The calibration graph was made using Fe (II) standard solution. The data are summarized in the **Table 3.15.** Linearity was verified 0.03 to 1.00 ppm in this range. Absorbance measurements were performed at the analytical wavelength 510 nm. The calibration curve of orange-red colored complex was observed as shown in **Figure 3.13**

Table 3.15 Calibration data of orange-red complex by the visible spectrophotometer

$[Fe^{2+}]$, ppm	Absorbance	
	Standard method 1	Standard method 2
0.03	0.007	0.004
0.05	0.008	0.005
0.10	0.011	0.007
0.25	0.025	0.022
0.50	0.046	0.041
0.75	0.071	0.066
1.00	0.088	0.087
Equation of linearity	y = 0.086x + 0.0036	y = 0.0867x - 4E-05
R-square (R^2)	0.9979	0.9982

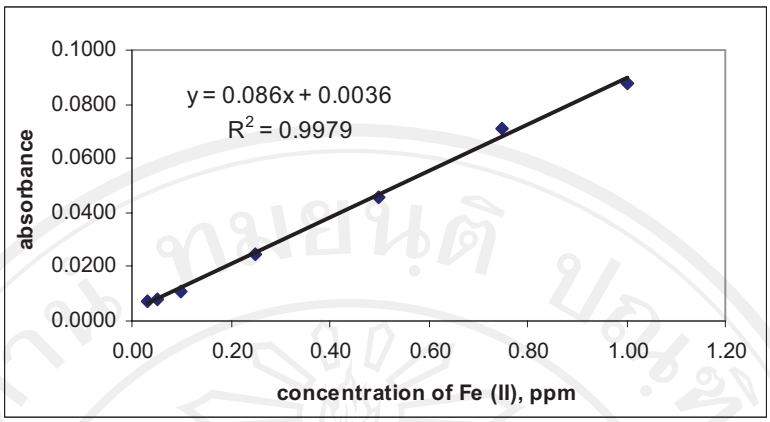

Figure 3.13 Calibration curve for Fe (II)

The calibration graph has positive slope because the amount of Fe (II) concentration was increased then, increasing the amount of absorbance was obtained. The orange-red complex solution obeys Beer's law in which intensity is independent of pH from 3 to 9. A pH between 2.9 and 3.5 will be rapidly colored development. In this experiment, a pH approximately 3.25 was used for preparation solution following to standard method. From the calibration graph, the equation of this linearity curve was obtained in which used for measuring quantity of Fe (II) in groundwater and water ponds. The results are presented in **Table 3.16**

Table 3.16 Determination of Fe (II) in groundwater and water ponds samples

Type of sample	Concentration of Fe (II), ppm
s1	n.d.
s2	18.14
s3	n.d.
s4	n.d.
s5	n.d.
s6	n.d.
s7 diluted 25 fold	7.51
s8	n.d.
s9	0.83
s10	n.d.

n.d. as no detected

3.3 Phosphate determination

3.3.1 Study of the reaction

There are many modification of determination phosphate. In this study, the experiment will be focused conceptual model of the original Murphy and Riley method by using ascorbic acid as reducing agent and acid strength. As shows in the below reaction scheme, the molybdenum blue complex is formed in an acidic environment its absorbance spectrum is based on the acidity. In order to high acidity condition will be have maximum rate of color formation.

$$PO_4^{3-} + 12MoO_4^{2-} + 27H^+ \longrightarrow H_3PO_4(MoO_3)_{12}\ \text{[Mo (VI) yellow]} + 12H_2O$$

Reducing agent (ascorbic acid)

$$H_3PO_4.10MoO_3.Mo_2O_5 \longrightarrow H_3PO_4.8MoO_3.2Mo_2O_5$$

Phosphomolybdenum blue [Mo (V) blue]

Ascorbic acid as reducing agent has advantage that less salt sensitive, but slow color development. So that the addition of antimony was used in which, it was a catalyst increase the rate of reduction complex as shows in the below reaction scheme. This reaction was selected.

$$PO_4^{3-} + 12MoO_4^{2-} + 27H^+ \longrightarrow H_3PO_4(MoO_3)_{12}\ \text{[Mo (VI) yellow]} + 12H_2O$$

Reducing agent (ascorbic acid) | Antimony potassium tartrate

$$H_3PSb_2Mo_{10}O_{40}$$

Phosphoantimonyl molybdenum blue [Mo (V) blue]

Ascorbic acid method was selected because this method is more suited for the range of 0.01 to 6 ppm for orthophosphate determination. But some samples have higher concentrations over the range of analysis, it can be diluted to appropriate with the experiment.

3.3.2 Simple LOC with fiber optic spectrophotometer

3.3.2.1 Optimization

A. Absorption spectrum

The optimum wavelength to monitor the phosphoantimonyl molybdenum blue complex has been widely used at 880 nm in the following the standard method. However wavelength of the proposed method at 880 nm may not be appropriate in this experiment. So the measurement the λ_{max} under the experimental conditions by obtaining the absorbance spectrum of 1.00 ppm of phosphate concentration was done. The λ_{max} of the standard solution was found to be approximately 680-730 nm. The spectrum of phosphoantimonyl molybdenum blue complex was observed as shown in **Figure 3.14**. This spectrum used 2.5 M H_2SO_4 by mixing in the combined reagent and to study in another effect in the experiment.

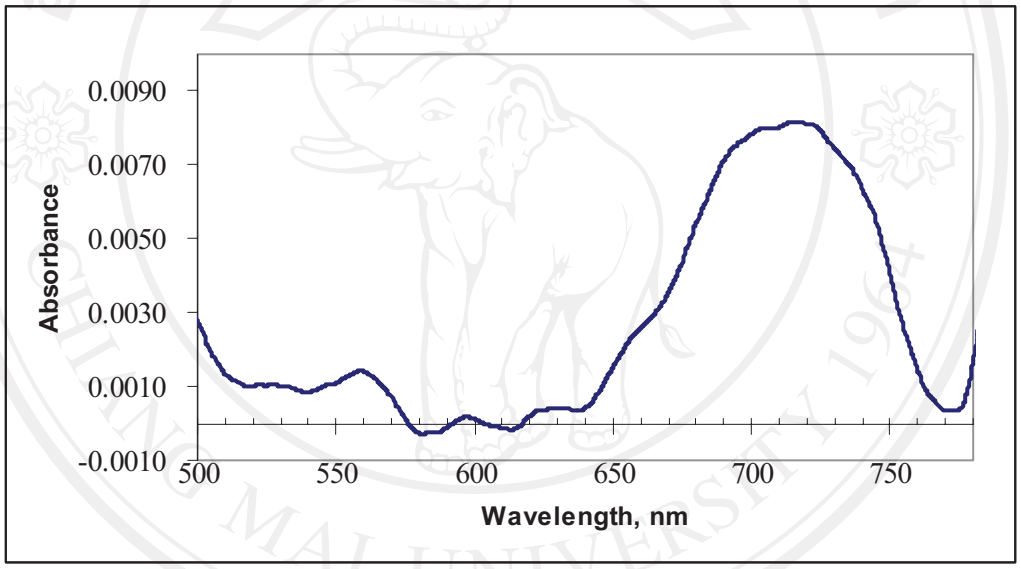

Figure 3.14 The spectrum of the phosphoantimonyl molybdenum blue complex in sulfuric acid 2.5 M (1.00 ppm of phosphate concentration)

P.J. Worsfold et al. [49] reported that under low acidity conditions, for example, non-linear color development and non-phosphate sensitized reduction (self-reduction of the molybdate) can occur. In the literature, a pH range of 0.57-0.88 suggested for optimum sensitivity (maximum rate of color formation).

This spectrum can be observed a wavelength maximum equal to 680-750 nm of range as blue color in which will be absorbed yellow color. This blue color was phosphoantimonyl molybdenum blue complex from Mo (V).

This condition was selected to determine phosphate in a pond water sample. In order that, offers other models of some parameters by comparing with the standard method and applied to quantitative analysis.

B. Elevator of the chip

In this experiment, the suitable elevator of the chip was investigated by comparing the differences of the migration time when tilting the chip 0, 10, 15, and 30 degree of elevator as respected to the horizontal plane. It can be seen **Figure 3.15**.

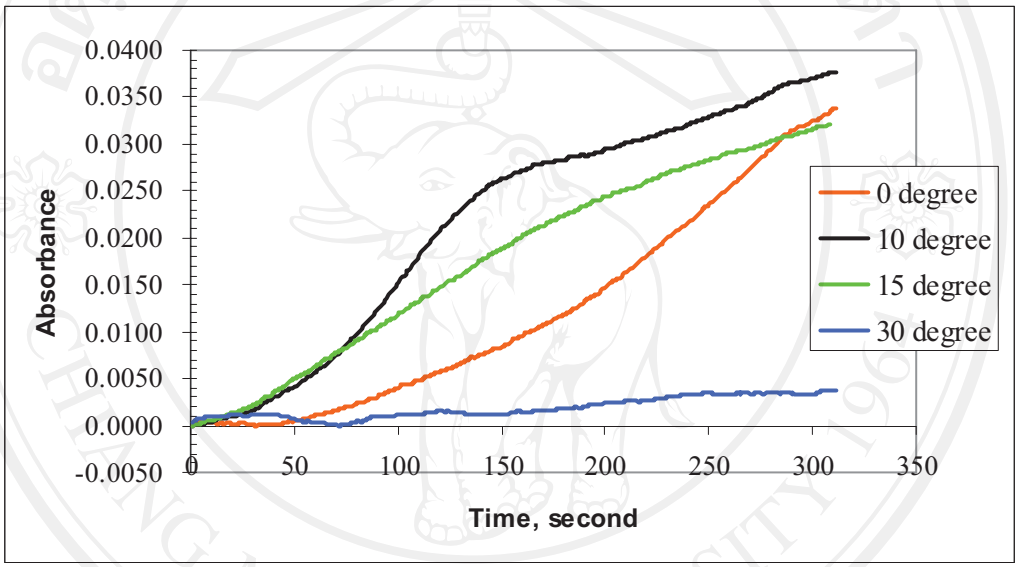

Figure 3.15 Effect of the elevator, the signal obtains from recording between absorbance against time containing 0, 10, 15, and 30 degree

In which, 5 ppm concentration of phosphate solution was pumped into the vertical channel and the combined reagent was pumped into the horizontal channel. The results were that migration of complex at 0 degree was not observed. In order to this reaction was slow the color formation. So, the elevator of the chip was tilted to 10 degree which, the signal will be increased rapidly until access to constant stage. This result was observed irregular signal when compared 15 degree that has performed regularly signal. This means the selective of elevator at 15 degree was obtained. In a part of 30 degree will appear the signal lower than another elevator which, the observation was unclear. This may be because the elevator of a chip was tilted more than 30 degree will not be completely measured.

C. The effect of the injection into the vertical or horizontal channels

To investigated the effect of injection into the vertical and horizontal channels phosphoantimonyl molybdenum blue complex in the following to type of injection. There are 2 set of type of injection using 15 degree of elevator, H_2SO_4 2.5 M, and a wavelength approximately 730 nm were selected.

- **The condition 1**, the phosphate concentrations were injected into the vertical channel and the combined reagent was injected into the horizontal channel. It was found that, the color formation of the complex increased rapidly until approximately 100 second. After which the signal will be slower changed of each phosphate concentrations as shown in **Figure 3.16**

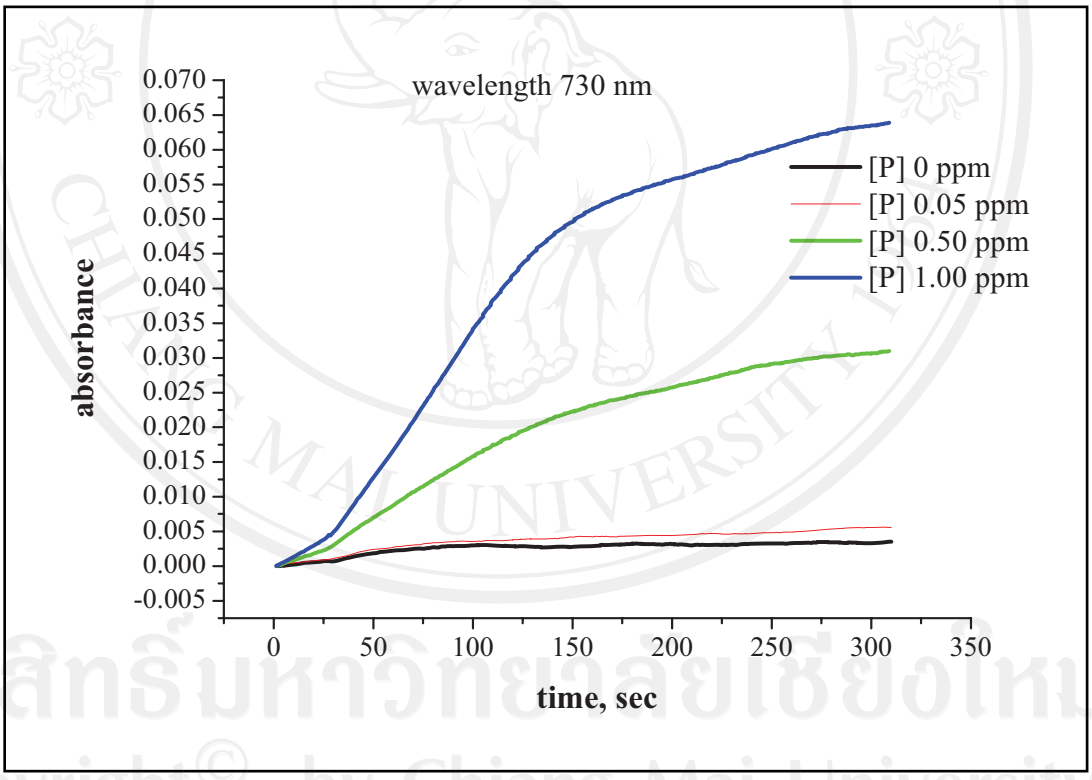

Figure 3.16 The signals of complex by plotting between absorbance and time

- **The condition 2,** the phosphate concentration was injected into the horizontal channel and the combined reagent (the same with the condition 1) was injected into the vertical channel. The result was shown in **Figure 3.17**

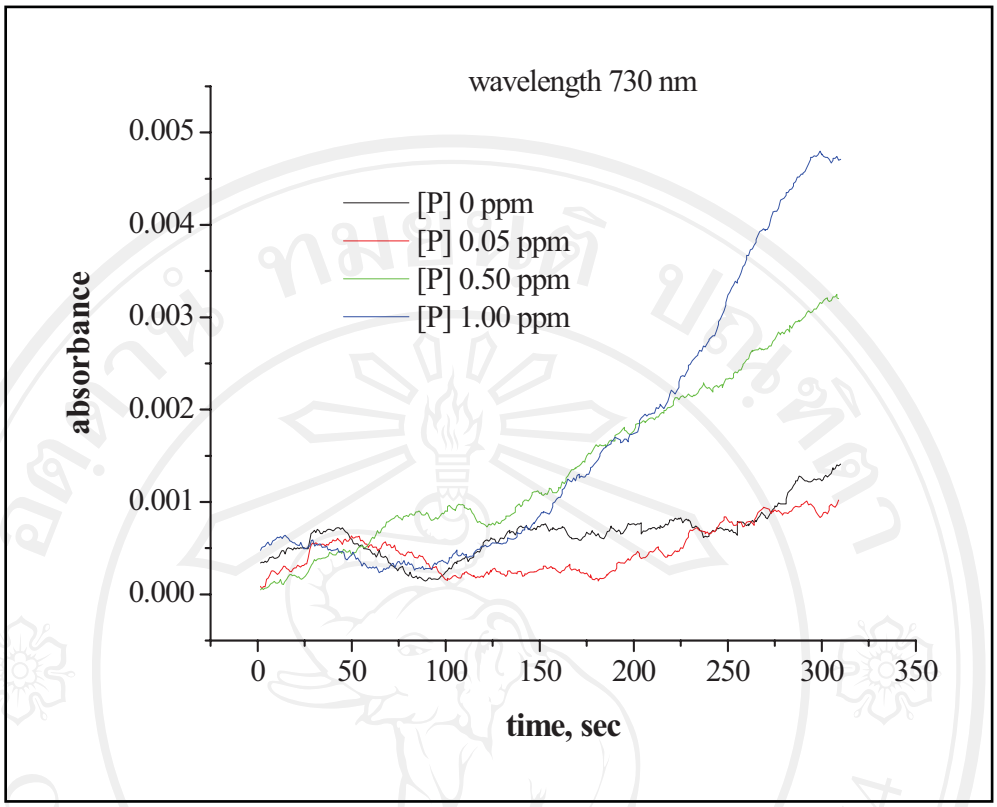

Figure 3.17 The signals of the condition 2 was obtained by plotting between absorbance and time

From the condition 2 was improved the injection channel by punctuating of the injection type. It was found that these results can not be observed the signal. In order to, it was not the most suitable for the migration and the reaction of these particular standard/combined reagent solutions. Therefore, the condition 1 was chosen in this experiment.

D. Effect of potassium antimonyl tartrate solution

The model compound standard was prepared in phosphate concentration (0.50 ppm) with the combined reagent with and without potassium antimonyl tartrate solution. Then this mixture solution was tested. **Figure 3.18** shown that the comparisons the effect of potassium antimonyl tartrate solution is greatly enhanced absorbance when time increased. In a part of the mixture solution did not add antimony, it was found that absorbance value was lower than added antimony. So that antimony has been affected for the complex, in addition antimony as a catalyst increases the rate of reduction of the complex. It was performed to catalyst the rate of

reaction to reach equilibrium. Moreover, antimony can be increased the sensitivity of analysis. And then, this effect of antimony in the proposed method was compared with the standard method. It was found that it have tended to the same of both methods.

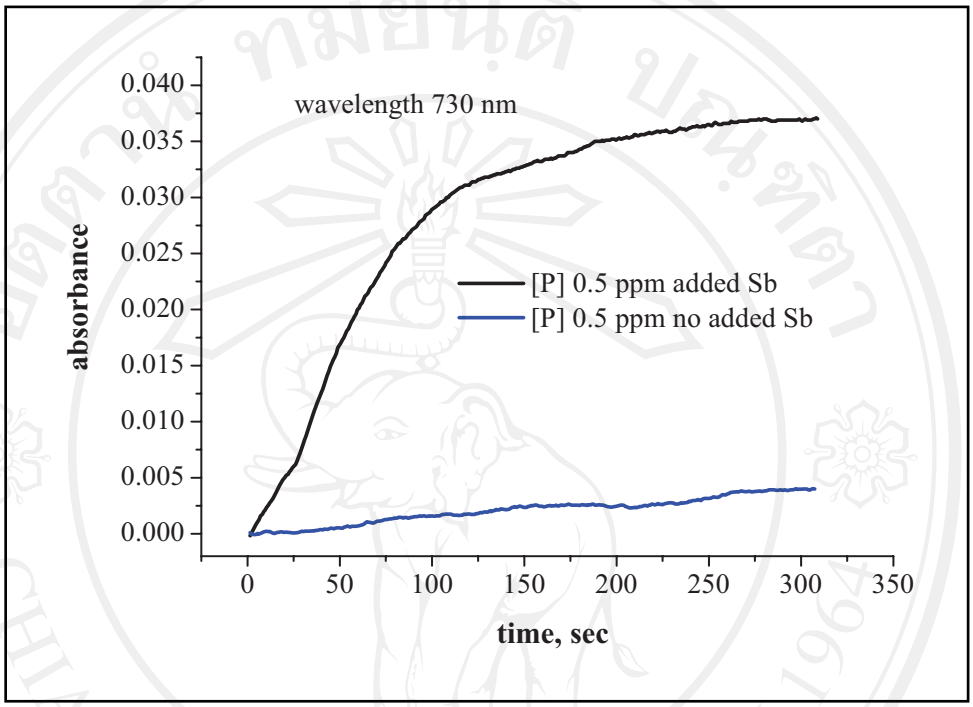

(**a**)

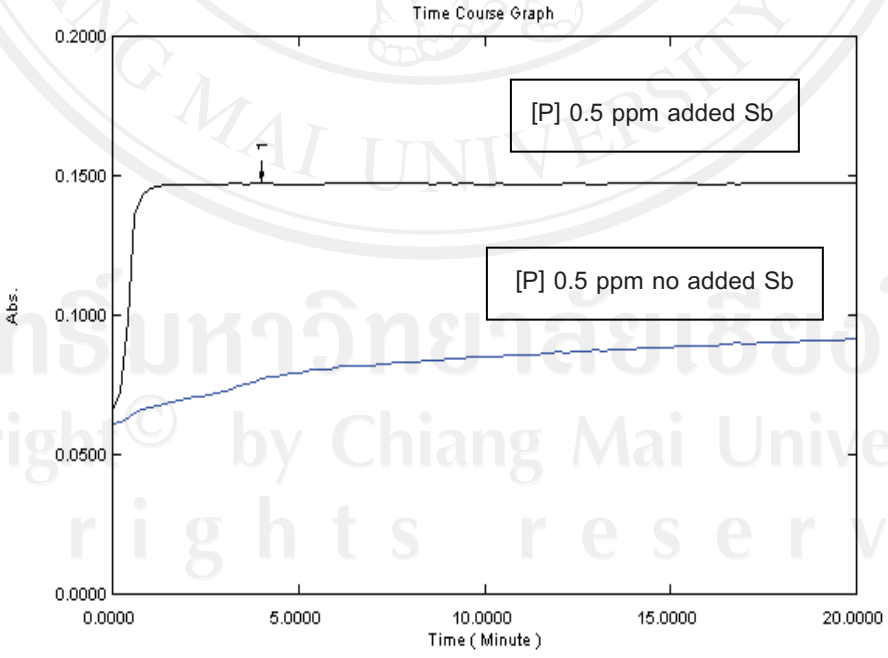

(**b**)

Figure 3.18 The comparisons of the effect of antimonyl; (a) The proposed method and (b) The standard method

3.3.2.2 Linearity of the calibration curve

Working calibration solution between 0.03 to 1.00 ppm was prepared from the stock standard solution. The ascorbic acid method is more suited for the range of 0.01-6.00 ppm. The linear calibration graph was selected under the chosen conditions were established by plotting absorbance against phosphate concentration as shown in **Table 3.17** and **Figure 3.19**. The ascorbic acid method can be determined quantity of phosphate in orthophosphate form. A wavelength approximately 680-780 nm of range was selected.

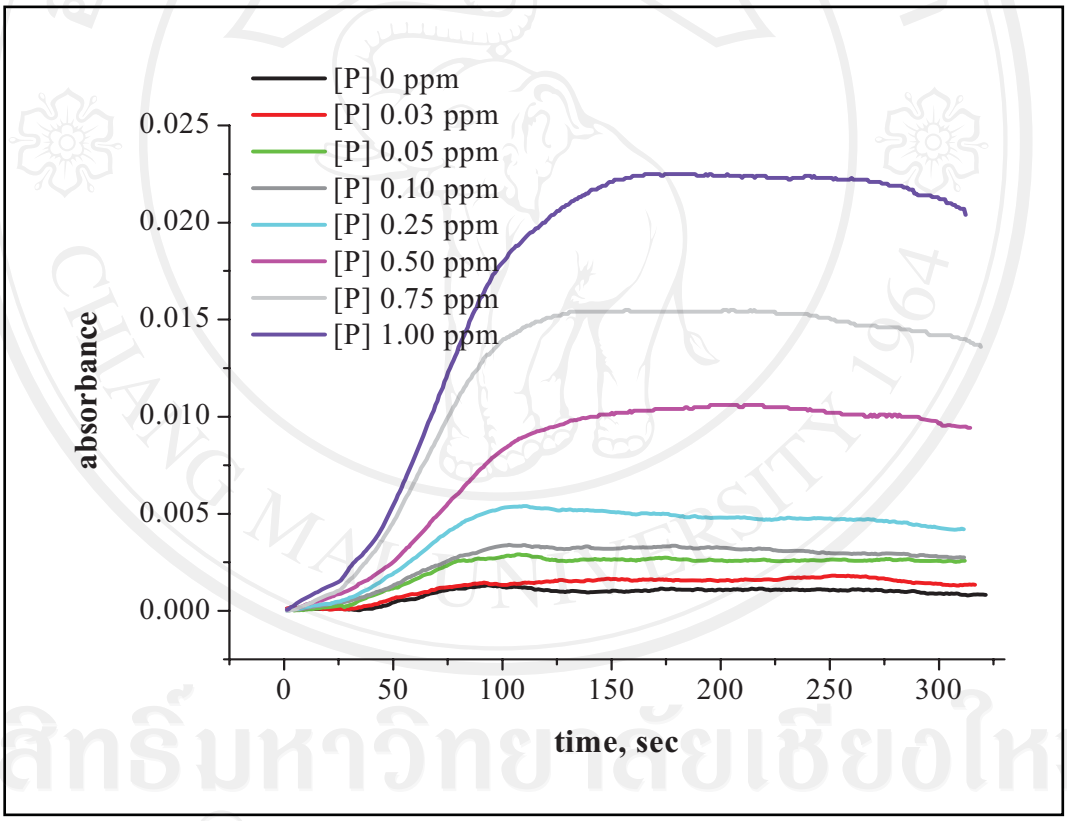

Figure 3.19 The signal of complex consists of all phosphate concentrations

Table 3.17 The signal of migration of orthophosphate for the use in real samples

Concentration of phosphate, ppm	Absorbance		Slope	
	150 sec	minus blank	60-70 sec	minus blank
0.00	0.0010	0.0000	3.63E-05	0.00E+00
0.03	0.0016	0.0006	2.79E-05	-8.43E-06
0.05	0.0027	0.0016	4.86E-05	1.23E-05
0.10	0.0032	0.0022	4.93E-05	1.30E-05
0.25	0.0050	0.0040	9.34E-05	5.70E-05
0.50	0.0102	0.0091	1.28E-04	9.21E-05
0.75	0.0156	0.0146	2.10E-04	1.74E-04
1.00	0.0230	0.0220	2.78E-04	2.42E-04

Notation: Standard deviation (SD) equal to 0.00

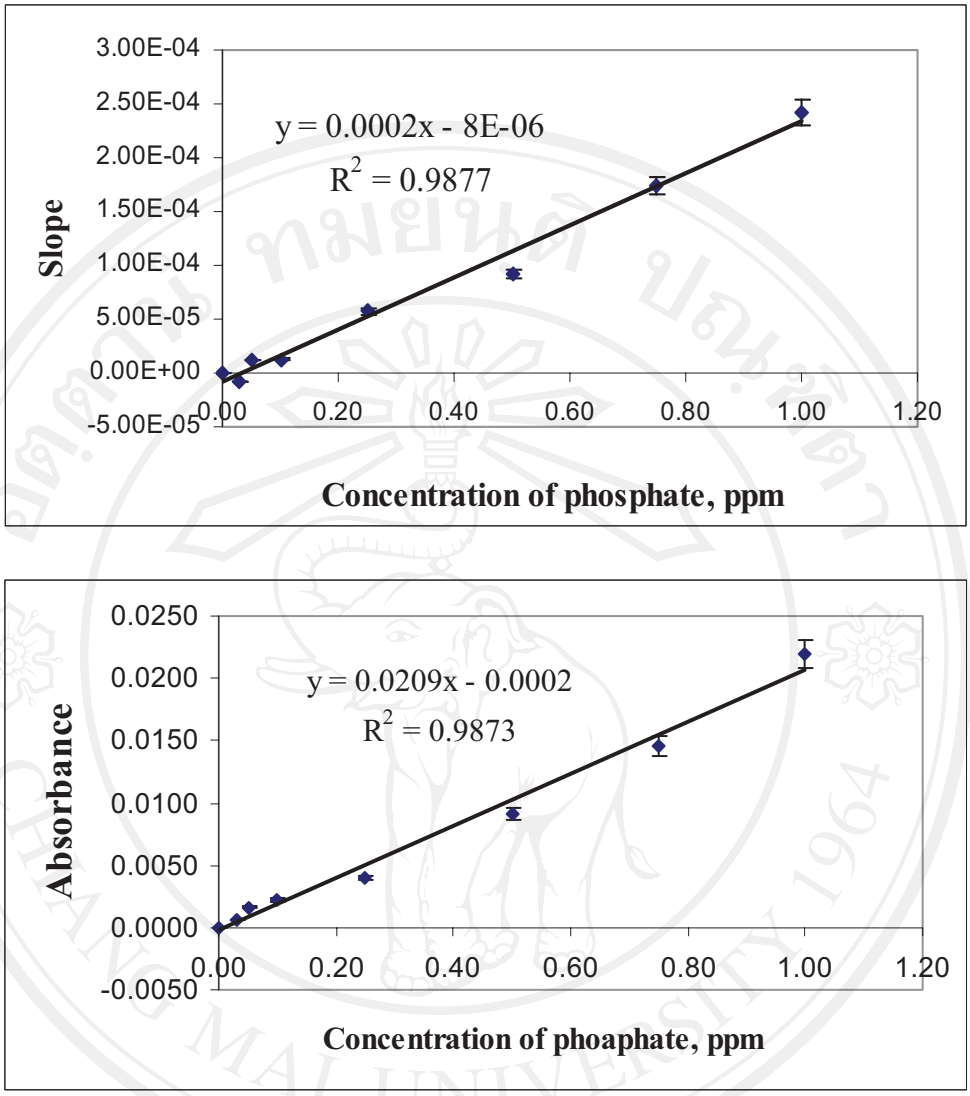

Figure 3.20 The calibration curve of the phosphoantimonyl molybdenum blue complex

In this calibration graph, the results have many of ranges of calibration graph by the analysis will be chosen to appropriate with sample.

The calibration graph has positive slope because the increasing of phosphate concentration increased the absorbance of the reaction zone. Due to the high concentration of phosphate will be formed the complex with the combined reagent too much. The intensity of blue color of the complex was the high intensity that absorbance will be increased. The measurement is based on the following theoretical model as Beer's law.

3.3.2.3 Evaluation of a simple LOC

In this study, analysis of orthophosphate in pond water samples were performed using a simple LOC system under operational conditions selected from optimization. The samples were prepared in acid-hydrolysis. Some samples have higher concentration over the calibration graph of range, it can be determined by diluting sample to appropriate with analysis of range. The results are summarized in **Table 3.18.**

Table 3.18 The determination of orthophosphate in pond water samples

Type of sample	Concentration of phosphate, ppm		
	The proposed method		The standard method
	Absorbance	Slope	
s1	0.04	0.04	0.03
s2	7.11	11.86	5.02
s3	0.16	0.22	0.17
s4	0.11	0.07	0.04
s5	0.74	1.05	1.03
s6	0.04	0.05	0.05
s7	0.03	0.04	0.04
s8	0.25	0.25	0.25

The results were obtained for all analytes with acceptable by considering percentage of different. Whereas some sample will have the effect of interference although, it can be eliminated in treatment of sample the following as the standard method. It may not be eliminated of all in order to the too high interference and affected with analysis.

3.3.2.4 Standard addition

Standard addition was assumed by plotting absorbance/slope against the final phosphate concentration (0, 0.05, 0.10, 0.50, and 1.00 ppm) under the selected conditions. This sample was used by adding 10 ml in 25 ml volumetric flask

so that, it has dilution factor equal to 2.5 to determine quantity of orthophosphate. The results were that the signals have tended to the same with the calibration graph which, is based on Beer's law.

Nevertheless, this result can be compared with the calibration graph to study the effect of interference and percentage of recovery. It was found that common interfering in some samples had no significant effect. In order to the effect of sample matrix on the formation of the complex was eliminated by adding concentrated H_2SO_4 for the preliminary sample treatment. And then, filtered sample immediately after collection. In addition to this sample was analyzed after fresh collection thus, phosphate concentration will not be decomposed.

The determination of orthophosphate from standard addition can be summarized as shown in **Figure 3.21.**

Figure 3.21 shows the signal of complex from standard addition method which, it was not performed sample 2 and 5. Because the signal had no the different of spiked each phosphate concentration. It may be affected of interference.

- **Sample 1**

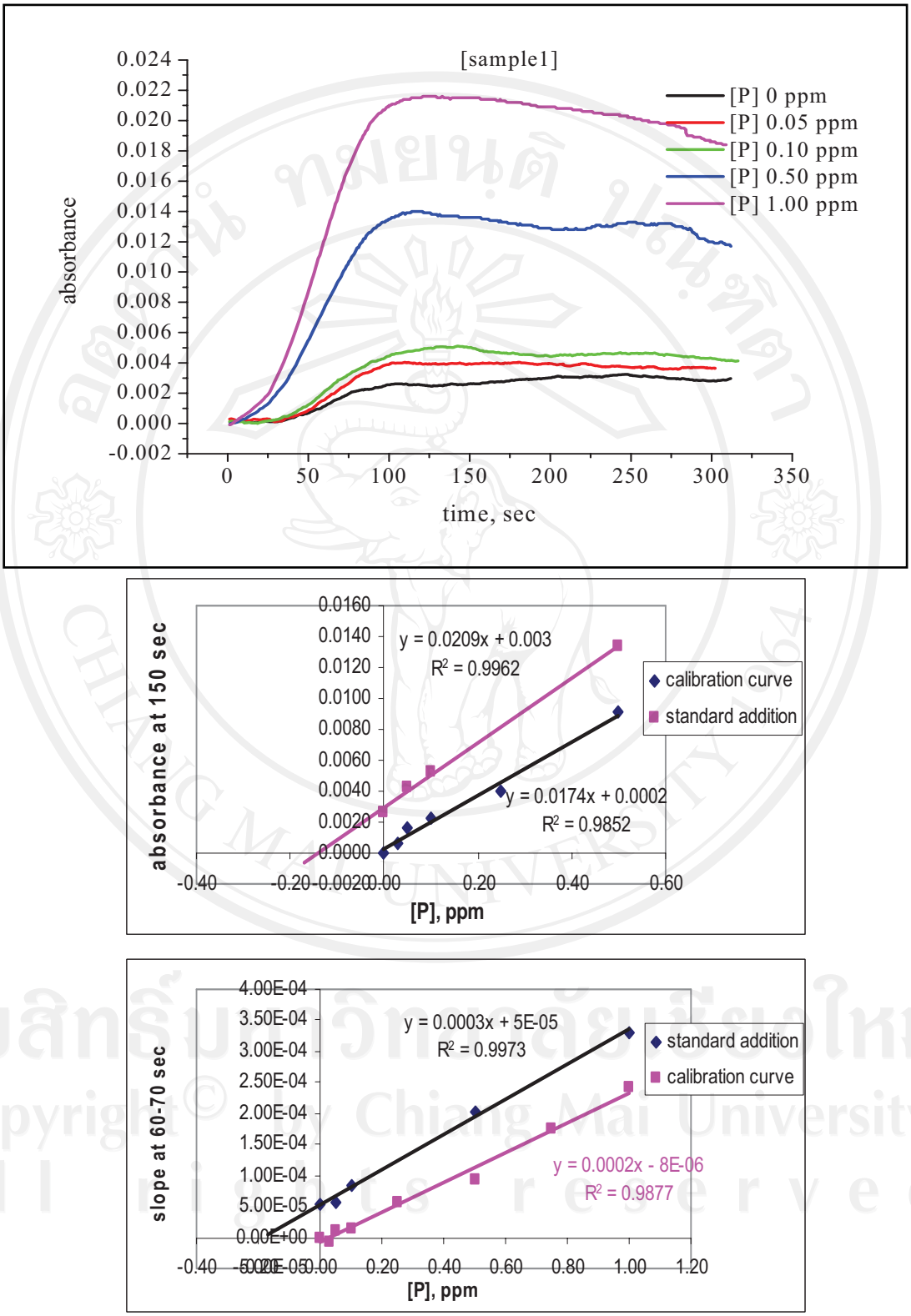

Figure 3.21 The signal of phosphoantimonyl molybdenum blue complex from standard addition in sample 1-8

- **Sample 3**

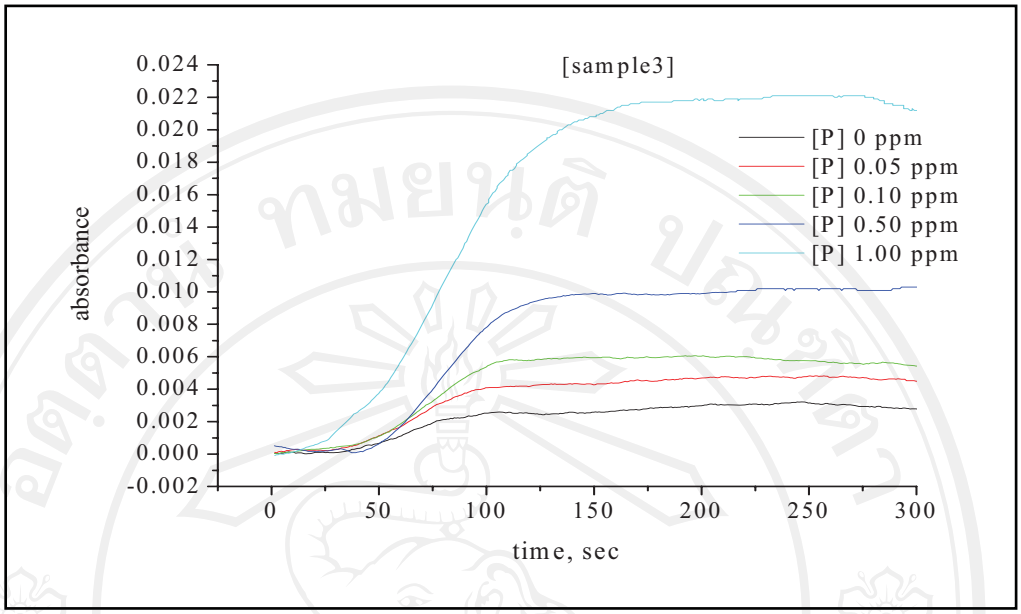

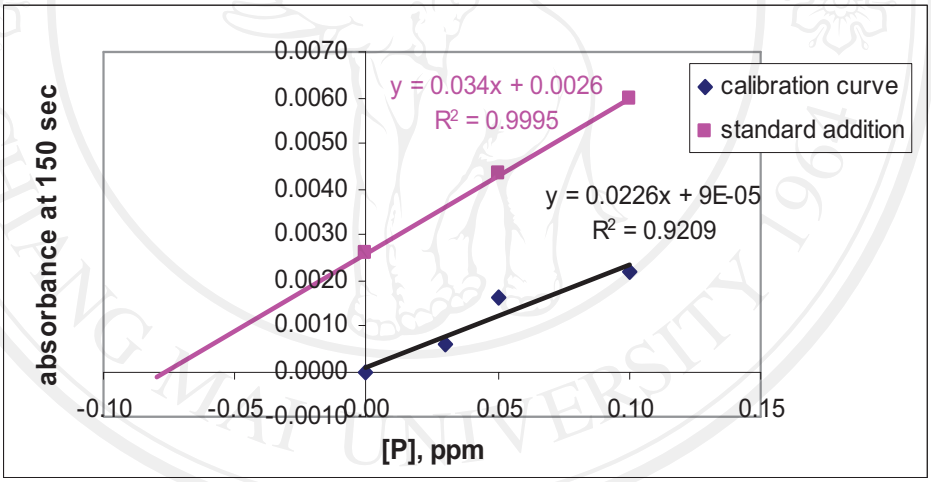

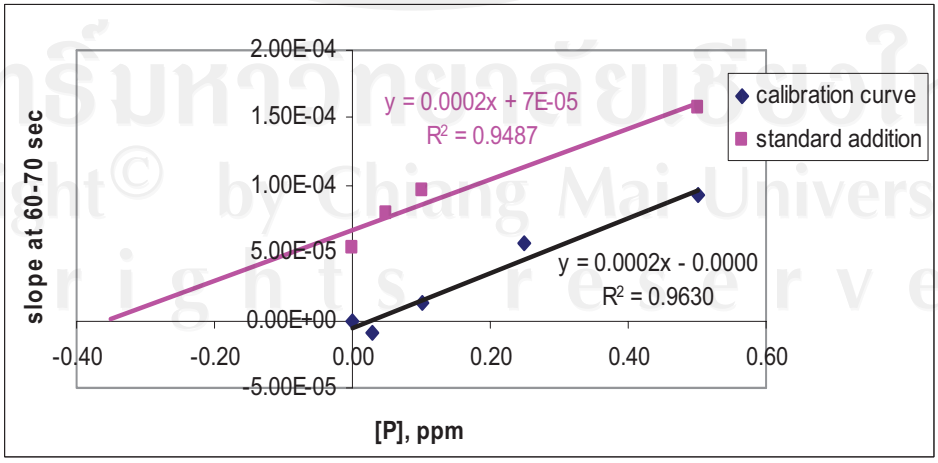

Figure 3.21 (continued)

- Sample 4

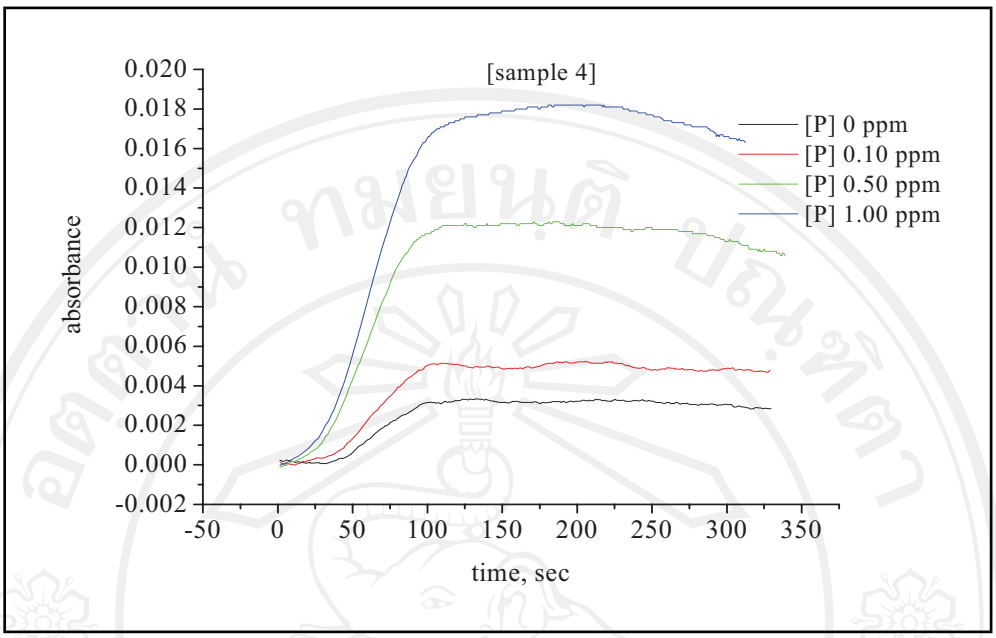

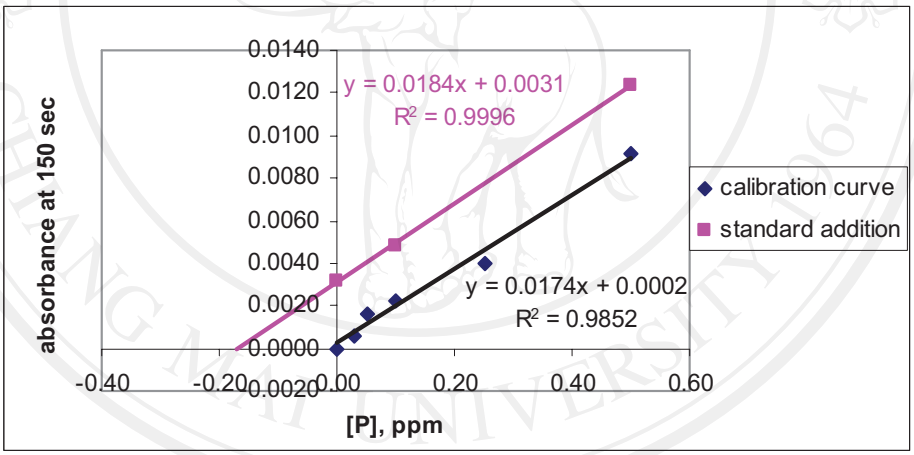

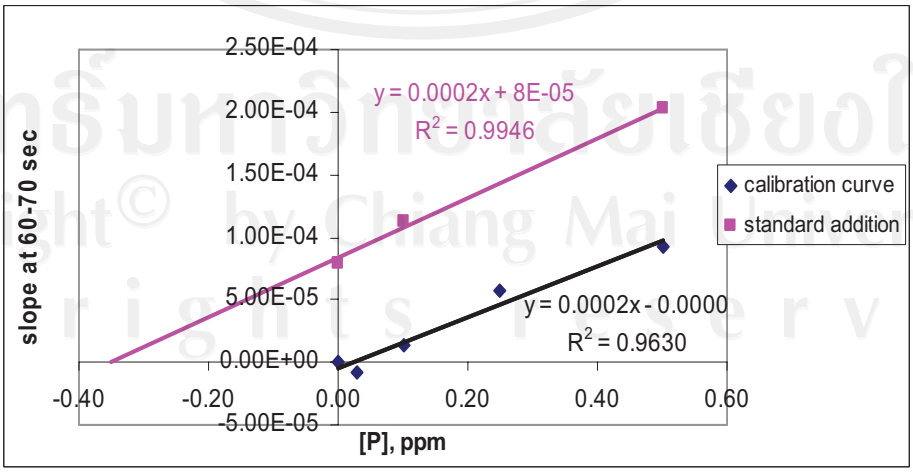

Figure 3.21 (continued)

- Sample 6

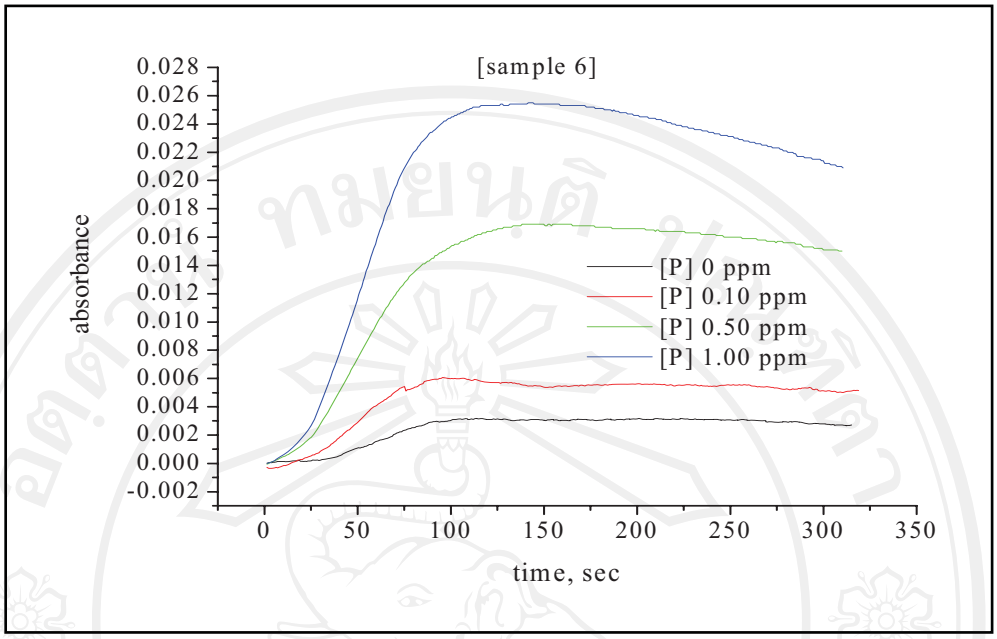

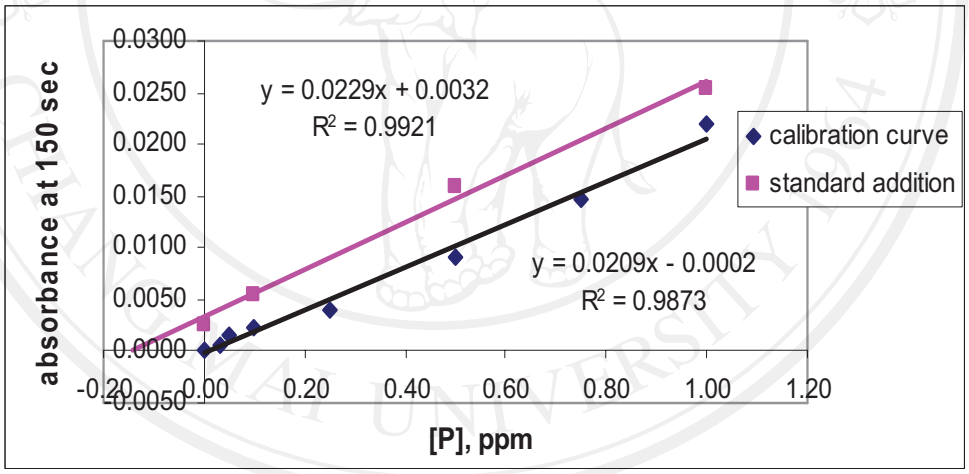

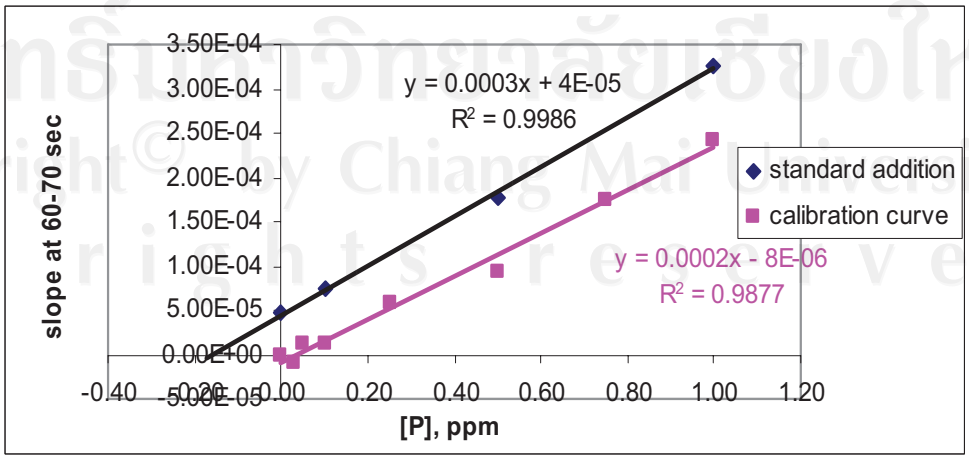

Figure 3.21 (continued)

- Sample 7

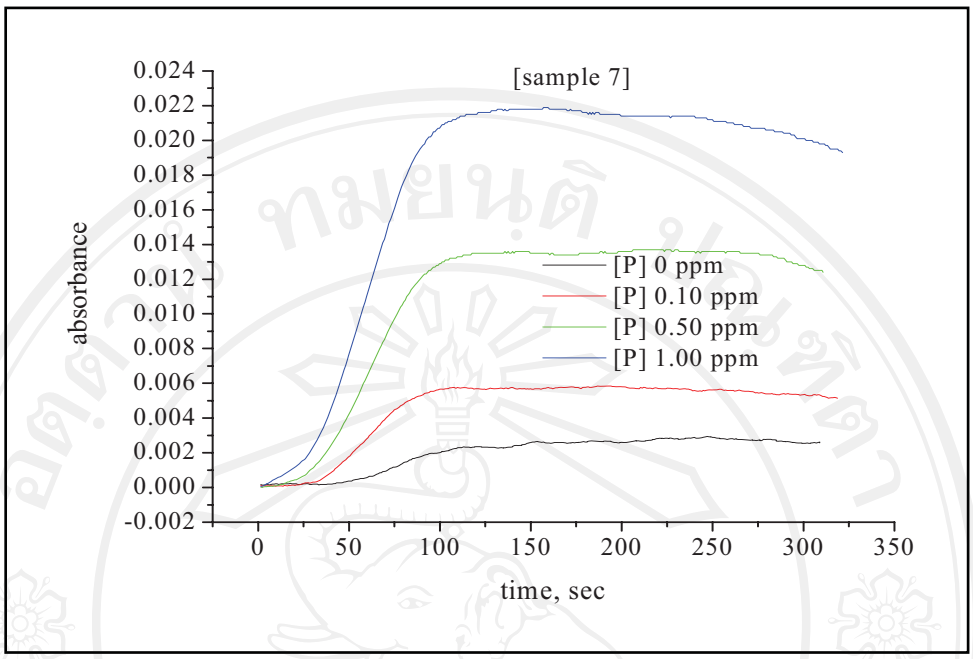

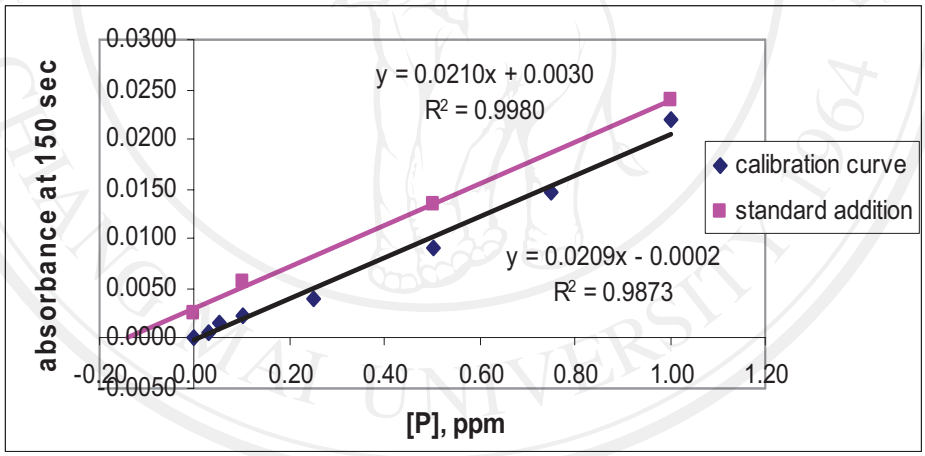

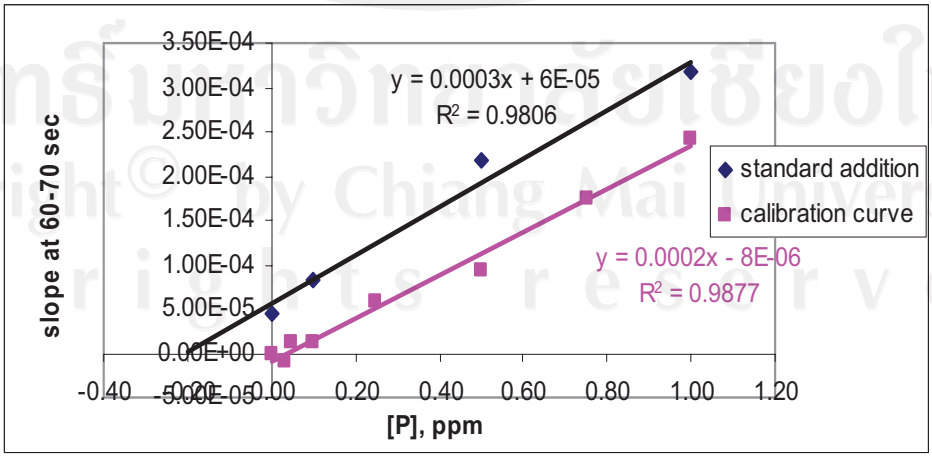

Figure 3.21 (continued)

- Sample 8

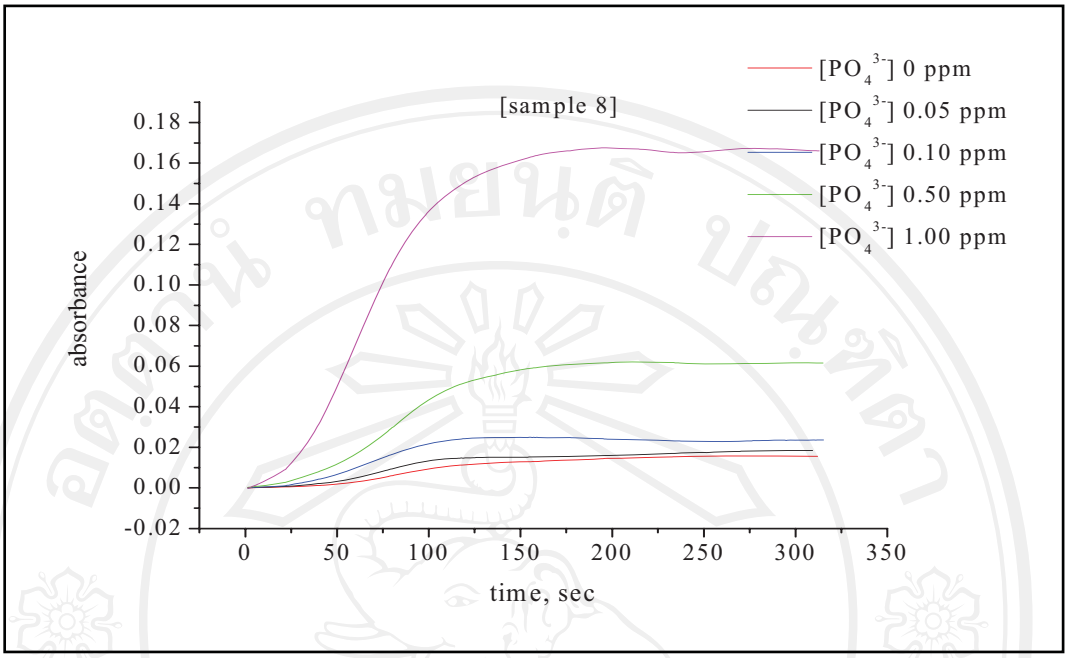

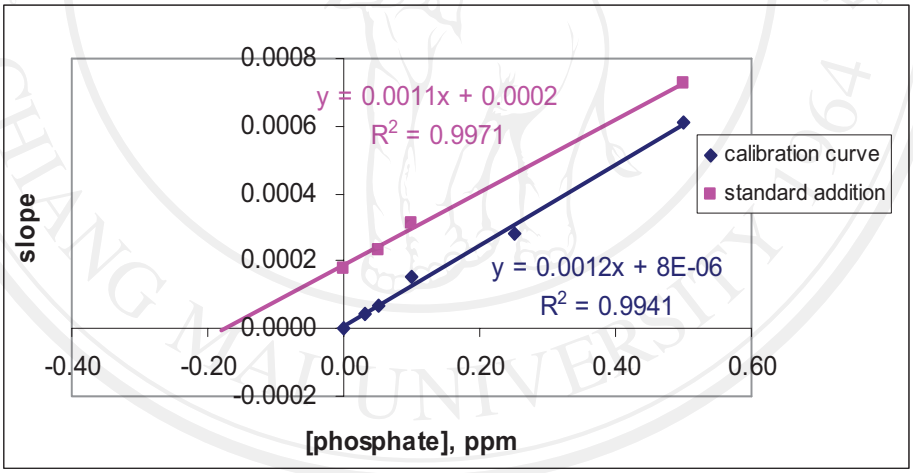

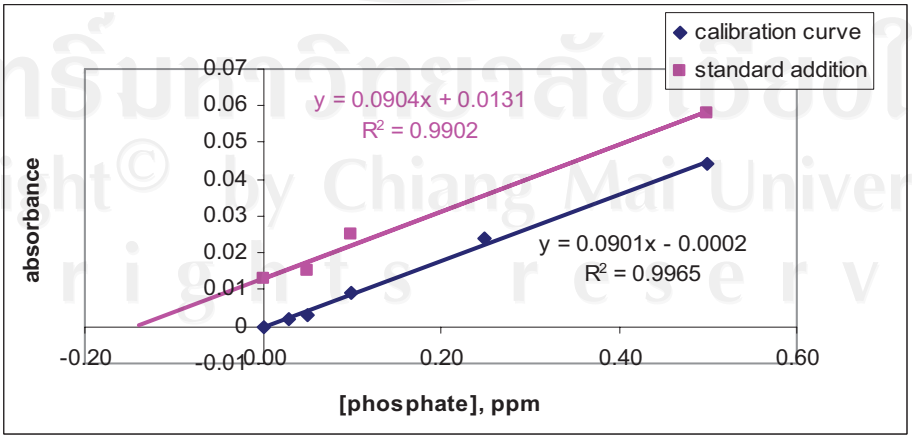

Figure 3.21 (continued)

Table 3.19 shows the determination of orthophosphate and percent recovery when spiked standard phosphate solution in real samples. The recoveries were 80-140%. It is unclear at this time for effect of interference. This interference may cause positive error in some pond water samples.

Table 3.19 Conclusion of percentage of recovery and quantitative of orthophosphate in pond water sample

Type of sample	Concentration of phosphate, ppm		% Recovery		Spiked standard, ppm
	Absorbance	Slope	Absorbance	Slope	
s1	0.43	0.43	108	138	1.00
s2	n.d.	n.d.	n.d.	n.d.	n.d.
s3	0.19	0.19	93	88	1.00
s4	0.42	0.42	105	123	0.50
s5	n.d.	n.d.	n.d.	n.d.	n.d.
s6	0.35	0.35	129	130	0.50
s7	0.36	0.35	103	137	1.00
s8	0.36	0.45	90	99	0.50

n.d. as no detected

3.3.3 Visible spectrometry

3.3.3.1 Calibration curve

The calibration data are listed in **Table 3.20**. The phosphate concentration was plotted at several concentrations and the different absorbance by measuring wavelength at 880 nm. The blue color of complex was observed as shown **Figure 3.22**

Table 3.20 The calibration data of visible spectrometry

Phosphate concentration, ppm	**Absorbance**	
	1	**2**
0.03	0.030	0.0110
0.05	0.053	0.0160
0.10	0.102	0.0310
0.25	0.253	0.0810
0.50	0.521	0.1670
0.75	n.d.	0.2480
1.00	0.972	0.3270
Equation of linearity	y = 0.9763x + 0.0078	y = 0.329x - 9E-06
R-square (R^2)	0.9987	0.9998

n.d. as no detected

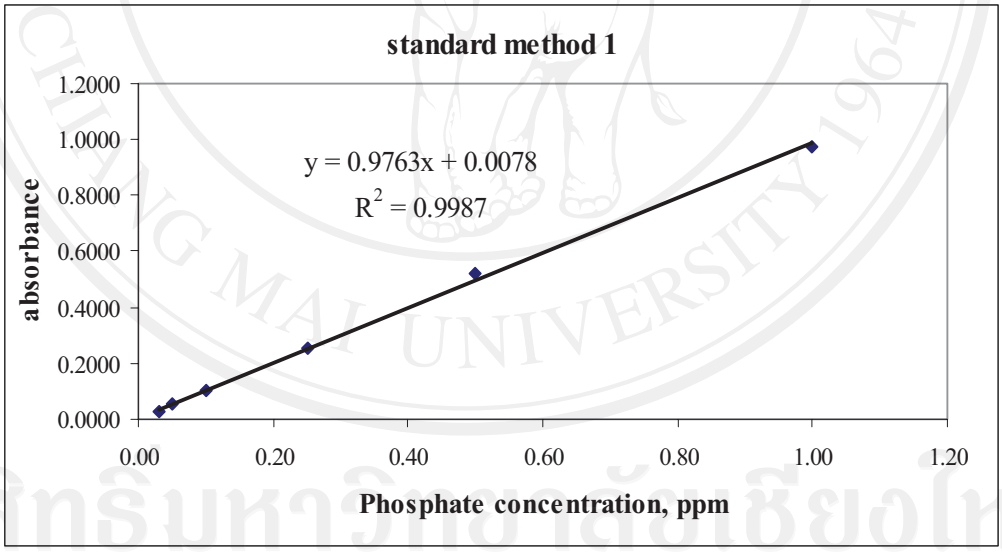

Figure 3.22 The calibration curve of the phosphoantimonyl molybdenum blue complex

Quantity phosphate in pond water samples are listed in **Table 3.21**

Table 3.21 Determination phosphate in pond water samples

Type of sample	Phosphate concentration, ppm
s1	0.03
s2	5.02
s3	0.17
s4	0.04
s5	1.03
s6	0.05
s7	0.04
s8	0.25